SINFONIA

Project title: Radiation risk appraisal for detrimental effects from medical exposure during management of patients with lymphoma or brain tumour (SINFONIA)

Grant Agreement: 945196

Call identifier: NFRP-2019-2020

Topic: NFRP-2019-2020-14 Improving low-dose radiation risk appraisal in medicine

Deliverable 3.5: Radiological assessment for human and aquatic wildlife

Lead partner:	SCK CEN (3)
Author(s):	Jordi Vives i Batlle, Lieve Sweeck and Fabricio Fiengo Pérez
Work Package:	3
Delivery as per Annex I:	Month 24 (27.02.2023)
Actual delivery:	Month 25 (23.02.2023)
Type:	Report
Dissemination level:	Public

Table of Contents

Abbreviations

CF	Concentration Factor
COMET	COordination and iMplementation of a pan-European instrumenT for radioecology
D-DAT	Dynamic Dose Assessment Tool
ERICA	Environmental Risk from Ionising Contaminants: Assessment and Management
FANC AFCN	Federaal Agentschap voor Nucleaire Controle or Agence fédérale de contrôle nucléaire
IAEA	International Atomic Energy Agency
ICRP	International Commission on Radiological Protection
INIS	International Nuclear Information System
K_d	Solid/liquid Distribution Coefficient
MODARIA	Modelling and Data for Radiological Impact Assessments
SCK CEN	StudieCentrum voor Kernenergie or Centre d'étude de l'énergie Nucléaire
7Q10	The 7-day low flow in a river that would be expected to occur every 10 years
$T_{1/2}$	Radioactive decay half-life
$T_{B1/2}$	Biological Half-life of Elimination
WWTP	Wastewater Treatment Plant

List of figures

List of tables

1 Executive summary

This project aims at developing a practical demonstration of an approach for the environmental impact assessment of radiopharmaceuticals released from medical facilities, considering both humans and the wildlife impacted by such releases. The previous deliverable report D3.4 (Fiengo Pérez et al., 2022) generated radionuclide dispersion simulation results and selected a specific scenario (radionuclide discharges in the Belgian Molse Nete River during the year 2018), to symbolise typical environmental conditions likely to be found at source and downstream from a hospital. Following from this work, we estimate in a simple way the transit of radiopharmaceuticals along the sewer/wastewater treatment plant system and the transfer and radiation dose to people and aquatic wildlife, using purposely developed radiological exposure models.
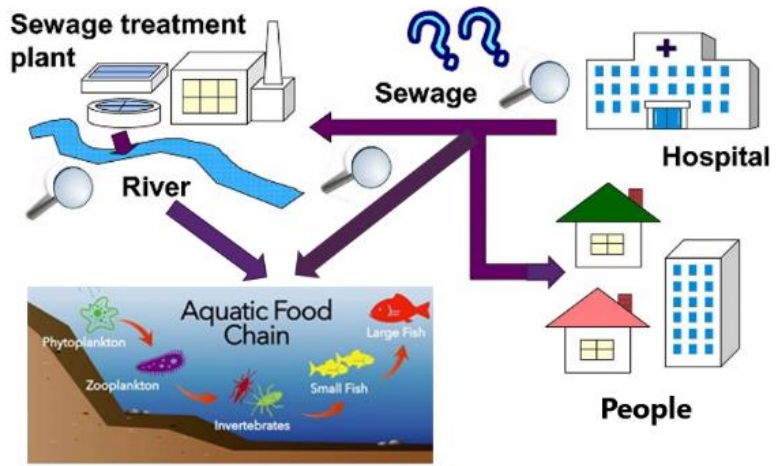
This study focusses on pollution of water and its incorporation to the food chain leading to human and wildlife exposure. We present a methodology to dynamic calculate dose rates to non-human biota at the outlet of a WWTP for short-lived hospital-sourced radionuclides, based on the redevelopment of the marine biokinetic model D-DAT (Vives Batlle et al., 2008; Vives i Batlle, 2016) for freshwater biota, and extending it to a wide range of medical radionuclides. We have also developed a method to calculate doses to WWTP workers and from agricultural practices in equilibrium conditions over a 1-year integration period. In this way, it has been possible to develop a conservative assessment method with limited number of modelling parameters, sufficiently realistic yet sufficiently simple to be practical for screening purposes.

All dose rates calculated in the example Molse Nete scenario are low. In the case of biota, they do not exceed the ERICA predicted no effects dose rate of 10 µGy h^{-1}. For humans, all dose rates for the different exposure pathways calculated are significantly below the 2.4 mSv y^{-1} public dose rate for all natural sources and below the 1 mSv y^{-1} limit for the public and workers in the non-nuclear industry, being also below a trivial level of dose rate (10 µSv y^{-1}) in most cases. Nevertheless, we recommend continuing to perform assessments of the impact of hospital radioactive releases to the people and the wildlife down the line, since they are still infrequent (because the primary focus is on exposure to patients) and exposures to medical radionuclides may increase with new nuclear therapies in the future. Along the way, methods should be improved to bring down uncertainty in model parameters such as biological transfer data for the radionuclides involved, separation efficiencies for different WWTP processes or dosimetry assumptions for external exposure to WWTP workers. This research is particularly important since discharges of radiopharmaceuticals in rivers are on the increase and it is necessary to explicitly demonstrate that people and the environment are adequately protected.

This project paves the way for a possible pan-European screening assessment methodology with the possibility to perform consistently assessments of the impact of radiopharmaceuticals on people and the environment.

2 Introduction

The objective of this project, designed as Task 3.3 within Work Package 3 of SINFONIA, is to show how to assess the impact of environmental releases of radiopharmaceuticals from hospitals on the public and the environment, using a Belgian test case as an example. This involves estimating radionuclide uptake in freshwater wildlife at the outlet of a WWTP and resulting uptake and internal/external exposures to aquatic wildlife for a given scenario. For the human part of the assessment, we considered human ingestion of aquatic biota and drinking of contaminated water after treatment in the WWTP, as well as external exposures at the riverbank and swimming, including also an indirect mechanism, namely internal doses arising from the consumption of agricultural foodstuffs after irrigation or fertilisation with contaminated sludge. The data on which this study is based are measurements from the Belgian Federal Agency for Nuclear Control (FANC), who performed a monitoring campaign at the outlet of several WWTPs receiving discharges from hospitals across the country. Atmospheric dispersion pathways are not included in this report because there are no measurements to back them up.

In the previous deliverable report D3.4 (Fiengo Pérez et al., 2022), we focused on the estimation of activity concentration in rivers after hospital releases and the selection of a test case to be used in the present radiological impact assessment. We incorporated the most relevant characteristics and conditions that could affect the fate and transport of radiopharmaceuticals in Belgian rivers exposed to hospital discharges, taking into account their decay half-lives, their distribution between solid and liquid phases, the volumes and activity levels, the discharge periodicity of the radioactive effluents and the flow regime of the receiving rivers.

In Belgium, there is a lack of radiological impact assessment of current as well as future medical releases and hospitals are not always forthcoming with information on their waste practices. This is because licensing usually does not require hospitals to sample or do monitoring of the environment and there is no notification procedure for outside releases. However, the activity concentrations in the Molse Nete River at the outlet of WWTP Mol are available and the dispersal pathways in that area are well understood, therefore constituting a most representative and conservative test for the pilot study in this project.

Using the available hydrometric data, D3.4 concluded that the year 2018 was one of the driest in the last decennia, especially in summer, leading to selecting this as the test case for subsequent study. The number of low flows around the minimum flow observed in 2018 is higher than in other years, justifying the selection of 2018 as the representative year for this study. With this information on hand, D3.4 assembled a one-year, 10 minute-interval time dataset of activity concentrations for ^{18}F, ^{123}I, ^{131}I, ^{153}Sm, ^{99m}Tc and ^{201}Tl at WWTP outlet (these are the radionuclides detected by the authorities), as well as a single spike ^{131}I accident scenario pertaining to the release of 1 MBq activity of ^{131}I due to accidental disposal of a radioactive pill to drain, as input to the present work.

The sequence followed to develop and execute the assessment method is as follows:

1. Devising a list of relevant radionuclides and creating a database of radioecological parameters for freshwater wildlife: expected chemical form, decay half-life, K_d, transfer factor and biological half-life information. We used mostly data from the ERICA assessment tool for wildlife impact assessment (Brown et al., 2008; Brown et al., 2013) and associated data collection approaches (Beresford et al., 2015b) where data was not directly available, including extrapolation methods to fill in the data gaps, since there was no experimental work foreseen in this project.

2. Adaptation of the Dynamic Dose Assessment Tool (D-DAT) model for marine wildlife (Vives Batlle et al., 2008; Vives i Batlle, 2016) to cover the freshwater environment, by re-parameterising the model with information from the aforesaid database and introducing the relevant radionuclides. This task included also the incorporation into D-DAT of a new human exposures post-processor to

calculate doses to people arising from the consumption of aquatic wildlife, or exposure to the contaminated water.

3. Literature review including examples of radiological assessment of liquid pharmaceutical discharges in sewers (McDonnell, 2004; Titley et al., 2000), leading to the production of a simple model to calculate doses to waste treatment plant workers, sewer maintenance workers and the public drinking the water and eating from the terrestrial foodchain. This model was customised with the relevant parameters for the Belgian situation and selecting the appropriate radionuclides.

4. Performance of the assessment calculations, interpretation of the results and discussion of lessons learned and recommendations for further research and development.

These steps are detailed in turn in the following sections of this report.

3 Database of radioecological parameters

A list of radionuclides was settled upon after searching the literature and consultation with the Belgian Regulator FANC, who provided measurement data (Fiengo Pérez et al., 2022). In the broadest possible sense our radionuclide parameters list may contain: ^{89}Zr, ^{90}Y, ^{99}Mo, ^{99m}Tc, ^{131}I, ^{131m}Xe, ^{133}Xe, ^{177}Lu, ^{177m}Lu, ^{223}Ra, ^{225}Ac, ^{226}Ra and ^{227}Th, although in practice this assessment covers only for ^{18}F, ^{123}I, ^{131}I, ^{153}Sm, ^{99m}Tc and ^{201}Tl because these are the only radionuclides detected in the vicinity of relevant Belgian WWTP outlets. Data for the remaining radionuclides is provided in readiness for future studies.

This database contains the following information: radionuclide chemical form, half-life, the solid-liquid distribution coefficient K_d, and the concentration factor CF and biological half-lives of elimination $T_{B1/2}$ for multiple processes. This information is displayed in Figures 1 and 2, covering general radionuclide information and biological half-lives, respectively.

We conducted reviews to obtain the information and we used a simple analogy with closest chemical element to complete gaps in the data. Since CFs for ^{99}Mo and ^{177}Lu could not be found in the ERICA database and extrapolation was not straightforward, we used a conservative value from another transition element for ^{99}Mo and a lanthanide for ^{177}Lu. We therefore followed this advice and decided on Tc as an analogue for Mo as it is the nearest transition metal in terms of closest atomic number.

For Lutetium, the situation is more difficult; ERICA has data for La, Ce and Eu with La and Ce having high K_ds and Eu behaving more as a soluble element. It is stated that K_ds for lanthanides vary in the order Eu < Ho < Gd < Er < Dy < La (Tomczak et al., 2019); clearly it is better to take a high value for Lu from among the lanthanides, which signals that our most appropriate analogue for Lu and Sm radionuclides is Eu. In similar fashion, we used Cl data as an analogue for F, given the closeness of these elements in the periodic table. For the CF and K_d specifically, additional sources of information and data extrapolation included data from the ongoing new revision of the IAEA SRS-19 report (IAEA, 2001), and other sources describing Tc uptake experiments for crustaceans and molluscs, performed at Oregon State University (Hevland, 1981; McKenzie-Carter, 1985). The thallium K_d is a sensitive parameter in our study, given the activities and retention times involved. Here, a single suitable source was found (Seaman and Kaplan, 2010). For the CR data gaps encountered for ^{201}Tl we used published measurement data (Zitko, 1975) for fish and we used Pb as an analogue for macroalgae.

PROJECT SINFONIA - DATABASE OF RADIONUCLIDE PARAMETERS FOR ENVIRONMENTAL IMPACT ASSESSMENT

Radionuclide information

Radionucl.	Relevance	Chemical form administered	Chemical form in the environment	Speciation category (based on K_d)	$T_{1/2}$ (s)	λ (d^{-1})	Kd (L kg^{-1})	Kd (m^3 kg^{-1})	Concentration ratio (Bq kg^{-1} FW per Bq m^{-3})					
									Fish	Crust.	Bivalve	Vasc. plant	Phytopl.	Zopl.
^{89}Zr	Used in positron emission tomography (PET); hospital releases	Radiolabeled monoclonal antibodies		Soluble	2.82E+05	2.12E-01	1.71E+05	1.71E+02	1.26E+00	8.20E-01	8.20E-01	9.71E-02	8.20E-01	1.51E+00
^{90}Y	Used in radiotherapy to treat cancer	injection of nanoparticulates/colloids labeled with $^{90}YCl_3$	Y^{+3} (ionic)	Soluble	2.30E+05	2.60E-01	4.00E+03	4.00E+00	7.90E-02	2.28E+00	2.28E+00	3.80E-01	2.28E+00	6.94E+00
^{99}Mo	^{99m}Tc production by decay of ^{99}Mo	Not administered		Highly soluble	2.37E+05	2.52E-01	2.59E+01	2.59E-02	9.90E-02	9.90E-02	9.90E-02	9.90E-02	9.90E-02	9.90E-02
^{99m}Tc	Nuclear medicine diagnostic procedures	$^{99m}TcO_4^-$ (VII), other reduced complexes in III or IV state	$^{99m}TcO_4^-$ (pertechnetate)	Highly soluble	2.16E+04	2.77E+00	2.59E+01	2.59E-02	9.90E-02	9.90E-02	9.90E-02	9.90E-02	9.90E-02	9.90E-02
^{131}I	^{99}Mo production byproduct, r unsealed source thyroid radiotherapy or diagnostic γ cameras; hospital releases	sodium iodide ($Na^{131}I$) and metaiodobenzyguanidine [2]	I^-	Moderately insoluble	6.93E+05	8.64E-02	1.14E+03	1.14E+00	3.10E-01	8.00E-02	8.00E-02	5.29E-02	8.00E-02	5.29E-02
^{131m}Xe	By-product of the ^{99}Mo production process	Noble gas (not administered)	As free element	Gas	1.02E+06	5.85E-02	0.00E+00	0.00E+00	0.00E+00	0.00E+00	0.00E+00	0.00E+00	0.00E+00	0.00E+00
^{133}Xe	By-product of the ^{99}Mo production process	Noble gas (not administered)	As free element	Gas	4.53E+05	1.32E-01	0.00E+00	0.00E+00	0.00E+00	0.00E+00	0.00E+00	0.00E+00	0.00E+00	0.00E+00
^{177}Lu	*Radiopharmaceutical percursor used for radiolabelling medicines; hospital releases*	*$^{177}LuCl_3$, Lutathera lutetium (177Lu)-oxodotreotide*	Akaline nature, $Lu(OH)_3$	Highly soluble	5.74E+05	1.04E-01	2.85E+05	2.85E+02	6.17E-02	1.59E+00	1.59E+00	2.19E-01	1.59E+00	8.32E+00
^{177m}Lu	*Radionuclide generator-based production of therapeutic ^{177}Lu from ^{177m}Lu*	Not administered	Akaline nature, $Lu(OH)_3$	Highly soluble	1.39E+07	4.32E-03	2.85E+05	2.85E+02	6.17E-02	1.59E+00	1.59E+00	2.19E-01	1.59E+00	8.32E+00
^{223}Ra	Xofigo therapy with ^{223}Ra dichloride injections to treat bone tumours	$^{223}RaCl_2$		Moderately soluble	9.88E+05	6.06E-02	8.47E+03	8.47E+00	1.04E+00	2.76E+01	5.23E+01	8.74E-01	5.23E+01	5.17E-01
^{225}Ac	*Targeted alpha-particle therapeutic applications for cancer treatment*	Free metal or various chelating and complexing agents		Highly insoluble	8.57E+05	6.99E-02	2.00E+07	2.00E+04	1.13E+00	3.35E+01	3.35E+01	4.44E+01	3.35E+01	1.19E+01
^{226}Ra	^{225}Ac production in medical linear accelerator (linac) by bombarding a ^{226}Ra target	Not administered	Insoluble	Moderately soluble	5.05E+10	1.19E-06	8.47E+03	8.47E+00	1.04E+00	2.76E+01	5.23E+01	8.74E-01	5.23E+01	5.17E-01
^{227}Th	*Targeted thorium conjugates(TTC)*	*Attached to targeting proteins such as antibodies for delivery to tumor cells*		*Highly insoluble*	1.62E+06	3.71E-02	2.68E+05	2.68E+02	7.17E-01	1.74E+01	1.74E+01	4.44E+01	1.74E+01	1.19E+01
^{18}F	*Fluorine-18 is one of the early tracers used in positron emission tomography (PET), having been in use since the 1960s.*	Sodium fluoride and fluorodeoxyglucose (FDG), where the 18F substitutes a hydroxyl.	F^-	*Soluble in the environment as F^-*	6.59E+03	9.09E+00	1.00E+00	1.00E-03	1.02E+00	1.02E+00	1.02E+00	2.78E-01	1.02E+00	2.78E-01
^{123}I	Used in nuclear medicine imaging, including single-photon emission computed tomography (SPECT) or SPECT/CT exams	usually supplied as sodium iodide in 0.1 M sodium hydroxide solution	I^-	Moderately insoluble	4.76E+04	1.26E+00	1.14E+03	1.14E+00	3.10E-01	8.00E-02	8.00E-02	5.29E-02	8.00E-02	5.29E-02
^{153}Sm	*Bone cancer palliation*	*As acomponent of samarium lexidronam.*	Chelated complex	*t is treated by the body in a similar manner to calcium, and it localizes selectively to bone.*	1.67E+05	3.59E-01	2.85E+05	2.85E+02	6.17E-02	1.59E+00	1.59E+00	2.19E-01	1.59E+00	8.32E+00
^{201}Tl	*Used in myocardial perfusion imaging (MPI) using either planar or single photon emission computed tomography (SPECT) techniques for the diagnosis and localization of myocardial infarction*	Thallous (I) chloride (TlCl) injection	Tl^+ (ionic)	Generally soluble. Tl has multiple oxidation states, hence variable sorption affinity. Tl(III) sorbs more strongly than Tl(I).	2.63E+05	2.28E-01	1.70E+03	1.70E+00	6.50E-01	9.79E-01	9.79E-01	4.73E-01	9.79E-01	8.61E-01

Colour coding for transfer parameters

Colour coding	Source of information
	IAEA live chart of nuclides (https://www-nds.iaea.org/relnsd/vcharthtml/VChartHTML.html)
	Using Tc as an analogue for Mo - nearest transition metal in terms of atomic number.
	Data from new revision of IAEA SRS-19 report
	Using Eu as an analogue for Lu and Sm as it maximises Kd for the three available candidates (La, Ce and Eu).
	Assumption of Kd = 0 and CR = 0 for noble gases
	Ac transfer factors from the new ERICA version, mostly extrapolated from Pu, Am and Th and some of the CRs are even based on data.
	Y transfer factors from the next ERICA version, originating from the wildlife transfer database 2020 version
	Primary value from current ERICA tool with or without extrapolation as below
	From direct sources describing uptake experiments: Data from McKenzie-Carter (1985) and Heveland (1981)
	Using Cl as an analogue for F
	Using Pb as analogue 9data from ERICA)
	Zitko et al (1975)

Figure 1: Screenshot of the database of radionuclide parameters (section 1: general radionuclide information)

Primary biological half-life information

Radionucl.	Biological half-life (d)					
	Fish	Crust.	Bivalve	Vasc. plant	Phytopl.	Zopl.
^{89}Zr				5.15E+00		
^{90}Y				5.15E+00		
^{99}Mo	3.40E+00	3.00E+00 (14.2%) 1.41E+02 (82.5%)	1.04E+02			3.00E+00 (14.2%) 1.41E+02 (82.5%)
^{99m}Tc	3.40E+00	3.00E+00 (14.2%) 1.41E+02 (82.5%)	1.04E+02			3.00E+00 (14.2%) 1.41E+02 (82.5%)
^{131}I	3.40E+00	3.00E+00 (14.2%) 1.41E+02 (82.5%)	1.04E+02			3.00E+00 (14.2%) 1.41E+02 (82.5%)
^{131m}Xe	0.00E+00	0.00E+00	0.00E+00	0.00E+00	0.00E+00	0.00E+00
^{133}Xe	0.00E+00	0.00E+00	0.00E+00	0.00E+00	0.00E+00	0.00E+00
^{177}Lu			2.00E+00 (61%) 3.40E+01 (39%)	2.70E+00	2.70E+00	
^{177m}Lu			2.00E+00 (61%) 3.40E+01 (39%)	2.70E+00	2.70E+00	
^{223}Ra	1.01E+01 (a) 2.66E+02 (b)	1.67E-01 (a) 4.30E+01 (b)	4.04E+03	6.94E-03 (a) 3.20E+00 (b)	6.94E-03 (a) 3.20E+00 (b)	2.50E-01 (a) 2.30E+00 (b)
^{225}Ac						
^{226}Ra	6.73E+00 (a) 4.95E+01 (b)	1.67E-01 (a) 4.30E+01 (b)	4.04E+03	6.94E-03 (a) 3.20E+00 (b)	6.94E-03 (a) 3.20E+00 (b)	2.50E-01 (a) 2.30E+00 (b)
^{227}Th	8.79E-01					
^{18}F						
^{123}I	0.00E+00	0.00E+00	0.00E+00			0.00E+00
^{153}Sm			2.00E+00 (61%) 3.40E+01 (39%)	2.70E+00	2.70E+00	
^{201}Tl						

Short biological half-life with data gaps completed

Radionucl.	Biological half-life (d)							Datagap filling comment
	Pel. Fish	Benth. Fish	Crust.	Bivalve	Vasc. plant	Phytopl.	Zopl.	
^{89}Zr	8.42E+00	8.42E+00	1.38E+00	2.00E+00	6.94E-03	6.94E-03	1.43E+00	Average of data available excl. actinides if possible
^{90}Y	8.42E+00	8.42E+00	1.38E-01	2.00E+00	6.94E-03	6.94E-03	1.43E+00	Same as Lutetium
^{99}Mo	8.42E+00	8.42E+00	3.00E+00	2.00E+00	6.94E-03	6.94E-03	3.00E+00	
^{99m}Tc	8.42E+00	8.42E+00	3.00E+00	2.31E+00	6.94E-03	6.94E-03	3.00E+00	
^{131}I	8.42E+00	8.42E+00	3.00E+00	2.31E+03	6.94E-03	6.94E-03	3.00E+00	
^{131m}Xe	0.00E+00	0.00E+00	0.00E+00	0.00E+00	0.00E+00	0.00E+00	0.00E+00	
^{133}Xe	0.00E+00	0.00E+00	0.00E+00	0.00E+00	0.00E+00	0.00E+00	0.00E+00	
^{177}Lu	8.42E+00	8.42E+00	1.38E+00	2.00E+00	6.94E-03	6.94E-03	1.43E+00	
^{177m}Lu	8.42E+00	8.42E+00	1.38E+00	2.00E+00	6.94E-03	6.94E-03	1.43E+00	
^{223}Ra	1.01E+01	1.01E+01	1.67E-01	4.04E+03	6.94E-03	6.94E-03	2.50E-01	
^{225}Ac	8.42E+00	8.42E+00	1.67E-01	4.04E+03	6.94E-03	6.94E-03	2.50E-01	Same as average for radium
^{226}Ra	6.73E+00	6.73E+00	1.67E-01	4.04E+03	6.94E-03	6.94E-03	2.50E-01	
^{227}Th	8.42E+00	8.42E+00	1.67E-01	4.04E+03	6.94E-03	6.94E-03	2.50E-01	Same as average for radium
^{18}F	8.42E+00	8.42E+00	3.00E+00	2.31E+03	6.94E-03	6.94E-03	3.00E+00	Same as iodine, since both are soluble
^{123}I	8.42E+00	8.42E+00	3.00E+00	2.31E+03	6.94E-03	6.94E-03	3.00E+00	Average of data available excl. actinides if possible
^{153}Sm	8.42E+00	8.42E+00	1.38E+00	2.31E+03	6.94E-03	6.94E-03	1.43E+00	Average of data available excl. actinides if possible
^{201}Tl	8.42E+00	8.42E+00	1.38E+00	2.31E+03	6.94E-03	6.94E-03	1.43E+00	Average of data available excl. actinides if possible

Long biological half-life with data gaps completed

Radionucl.	Biological half-life (d) - if single value, then it is the long component							Datagap filling comment
	Pel. Fish	Benth. Fish	Crust.	Bivalve	Vasc. plant	Phytopl.	Zopl.	
^{89}Zr	6.92E+01	6.92E+01	8.50E+01	6.90E+01	5.15E+00	2.70E+00	6.17E+01	Average of data available excl. actinides if possible
^{90}Y	6.92E+01	6.92E+01	8.50E+01	3.40E+01	5.15E+00	2.70E+00	6.17E+01	Same as lutetium
^{99}Mo	3.40E+00	3.40E+00	1.41E+02	1.04E+02	3.56E+00	2.70E+00	1.41E+02	
^{99m}Tc	3.40E+00	3.40E+00	1.41E+02	1.04E+02	3.56E+00	2.99E+00	1.41E+02	
^{131}I	3.40E+00	3.40E+00	1.41E+02	1.04E+02	3.56E+00	2.99E+00	1.41E+02	
^{131m}Xe	0.00E+00	0.00E+00	0.00E+00	0.00E+00	0.00E+00	0.00E+00	0.00E+00	
^{133}Xe	0.00E+00	0.00E+00	0.00E+00	0.00E+00	0.00E+00	0.00E+00	0.00E+00	
^{177}Lu	6.92E+01	6.92E+01	8.50E+01	3.40E+01	2.70E+00	2.70E+00	6.17E+01	
^{177m}Lu	6.92E+01	6.92E+01	8.50E+01	3.40E+01	2.70E+00	2.70E+00	6.17E+01	
^{223}Ra	2.66E+02	2.66E+02	4.30E+01	4.04E+03	3.20E+00	3.20E+00	2.30E+00	
^{225}Ac	1.58E+02	1.58E+02	4.30E+01	4.04E+03	3.20E+00	3.20E+00	2.30E+00	Same as average for radium
^{226}Ra	4.95E+01	4.95E+01	4.30E+01	4.04E+03	3.20E+00	3.20E+00	2.30E+00	
^{227}Th	8.79E-01	8.79E-01	4.30E+01	4.04E+03	3.20E+00	3.20E+00	2.30E+00	Same as average for radium
^{18}F	3.40E+00	3.40E+00	1.41E+02	1.04E+02	3.16E+00	2.99E+00	1.41E+02	Same as iodine, since both are soluble
^{123}I	3.40E+00	3.40E+00	1.41E+02	1.04E+02	3.20E+00	2.99E+00	1.41E+02	Average of data available excl. actinides if possible
^{153}Sm	6.92E+01	6.92E+01	8.50E+01	3.40E+01	2.70E+00	2.70E+00	6.17E+01	Average of data available excl. actinides if possible
^{201}Tl	6.92E+01	6.92E+01	8.50E+01	2.35E+03	3.36E+00	3.07E+00	6.17E+01	Average of data availableexcl. actinides if possible

Values in red are extrapolated from a related species (plant to phytoplankton or crustacean to zooplankton) or radionuclide analogues (Y as analogue for Ze)

Colour coding for biological half-lives

Colour coding	Source of information
	Data from McKenzie-Carter (1985) and Heveland (1981)
	Using Tc as an analogue for Mo - nearest transition metal in terms of atomic number.
	Using tdata from Blaylock and Frank (1981) for carp (Cyprinus carpio) and mosquitofish (Gambusia affinis)
	Assumption of 0 for noble gases
	Taking Ce as analogue and using aMODARIA WG8 Biological half-life database (http://dx.doi.org/10.1016/j.jenvrad.2015.08.018)
	Direct average from MODARIA WG8 Biological half-life database (http://dx.doi.org/10.1016/j.jenvrad.2015.08.018)
	Mahmood et al. (2014) https://www.google.com/url?sa=
	Assume same values for Eu, Lu and Sm
	Data from Seaman and Kaplan (2010):

For F and Sm we use Cl and Eu as analogues

Figure 2: Screenshot of the database of radionuclide parameters (section 2: biological half-lives)

The principal source available for the biological half-lives is the freely available international database of radionuclide biological half-life values developed during the IAEA project MODARIA (https://www-ns.iaea.org/projects/modaria/modaria2.asp?s=8&l=129, which includes 1907 entries for 52 elements for terrestrial, freshwater, riparian and marine organisms (Beresford et al., 2015a). Additional biological half-lives were researched in the IAEA INIS database (https://www.iaea.org/resources/databases/inis), with some success for direct data for lanthanides and thorium. We also performed gap extrapolation by finding the nearest radionuclide or biological analogues as described previously (these data are appropriately colour-coded in the database).

In some cases, our scientific judgement indicated that it was more adequate to use information from other sources not linked to the IAEA biological half-life database because additional literature was more suitable. In addition we used data for carp (*Cyprinus carpio*) and mosquitofish (*Gambusia affinis*) (Blaylock and Frank, 1981). For thorium in fish, we used additional data (Mahmood et al., 2014).

The extrapolation method indicated above, based on consideration of nearest chemical analogue, has the potential to be improved in future using chemical speciation knowledge. For example, iodate could be used to predict the long-term behaviour of ^{99}Tc, which is present in the aquatic environment mainly as the pertechnetate ion TcO_4^-.

4 Adaptation of the D-DAT model for freshwater assessments

4.1 Brief description of the D-DAT model

The D-DAT assessment model (Vives i Batlle et al., 2008) is a modelling tool that calculates wildlife concentrations (fish, crustaceans, molluscs, macroalgae, phytoplankton and zooplankton) using time series of contaminated water concentrations (measured or modelled) as input. It contains a sediment sub-model that considers suspended particulates, molecular diffusion, pore water mixing and bioturbation, in order to dynamically calculate sediment activity concentrations and therefore external dose rates to wildlife arising from sediment exposure, additionally to dose rates from internally incorporated radionuclides. This model has been successfully applied to Fukushima studies (Vives i Batlle et al., 2018) and was further developed into an advanced version which was the offspring of the Euratom project COMET (Vives Batlle, 2013; Vives i Batlle et al., 2018). The model implements a dual $T_{B1/2}$ approach, requiring three compartments: water (A_W), as well as a fast (A_{OF}) and slow (A_{OS}) organism compartments linked to fast and slow routes of uptake and release, respectively, which are governed by the following differential equations:

$$\frac{dA_W}{dt} = -(K_{Wf} + K_{WS} + \lambda)A_W + \frac{m}{V}(K_{OF}A_{OF} + K_{OS}A_{OS})$$

$$\frac{dA_{Of}}{dt} = K_{WF}\frac{m}{V}A_W - (K_{Of} + \lambda)A_{OF}; \frac{dA_{Os}}{dt} = K_{WS}\frac{m}{V}A_W - (K_{OS} + \lambda)A_{OF}$$

Where K_{ij} are the rate constants governing transfer from compartment *i* to compartment *j* (where *i* and *j* symbolise the water, organism-fast and organism-slow retention phases W, OF or OS), λ is the radionuclide decay constant, m is the mass of the organism, V is the volume of the water compartment with $K_{Of} = \frac{ln(2)}{T_{B1/2}^F}$ and $K_{Os} = \frac{ln(2)}{T_{B1/2}^S}$ (where $T_{B1/2}^F$ and $T_{B1/2}^S$ are the two "fast" and "slow" biological half-lives of elimination which can, in the general case, be present simultaneously). The exchange of radionuclides between water and sediment is represented by the dynamic coupling of the above model with a four-compartment (water and 3 layers of sediment) linear, first order kinetic exchange model (Lepicard et al., 2004; Lepicard et al., 1998; Simmonds et al., 2004) which includes the processes of particle scavenging, molecular diffusion, particle mixing, pore water mixing and sedimentation.

To calculate internal and external dose rates to the wildlife for the various radionuclides, activity concentrations (sum of the "slow" and the "fast" component) are multiplied by dose coefficients (μGy.h^{-1} per Bq.kg^{-1}) for the required organism, using published ICRP Publication 136 (ICRP, 2017) dose

coefficients, or DCs. External dose rates are calculated similarly by using external exposure DCs and purposely-defined occupancy factors, accounting for hybrid exposure from both water and sediment.

The D-DAT model is currently implemented in the ModelMaker® 4 modelling platform (Adamatzky, 2001; Citra, 1997; Rigas, 2000) and, in this form, it has had a very successful track record of application to a variety of environmental situations involving non-continuous discharges of radionuclides in the marine environment, as well as having been successfully tested in inter-comparisons with other dynamic models (Vives Batlle et al., 2008; Vives i Batlle, 2016; Vives i Batlle et al., 2016).

The Ability of D-DAT to balance incoming activity concentrations of radionuclides in water at the wildlife receptor location, combined with the explicit modelling of the role of sediments as a potential dose-giving reservoir of radionuclides, means that D-DAT is eminently suitable for adaptation to a freshwater environment. In this study, such conversion was carried out, together with extension from the original radionuclide set (the model was designed for the long-lived radionuclides ^{90}Sr, ^{99}Tc, ^{129,131}I, ^{134,1237}Cs, ^{239,240}Pu, ^{241}Am and ^{236}U) to the short-lived medical radionuclides considered in this study.

4.2 Adaptation of D-DAT to radionuclides in freshwater at the outlet of a WWTP

The D-DAT model performs simultaneous calculations for a suite of radionuclides, rather than calculating one radionuclide at a time. This is possible thanks to a very compact form of the model's differential equations, which are indexed as a two-dimensional array, with the first index i signifying the radionuclide and the index j signifying the wildlife group. In this compact format, the model's parameters are stored in compact form in a matrix format (and in the case of water concentrations, as a mono-dimensional array). Therefore, the first step in the adaptation of D-DAT for freshwater was the re-indexing of all the compartments and fluxes of the model. The reconfigured structure is shown in Fig. 3, which shows the upper level of the model structure, with the double-rectangle boxes signifying sub-models that can be "opened" in turn to reveal the different processor modules (see Figs. 4 – 7).
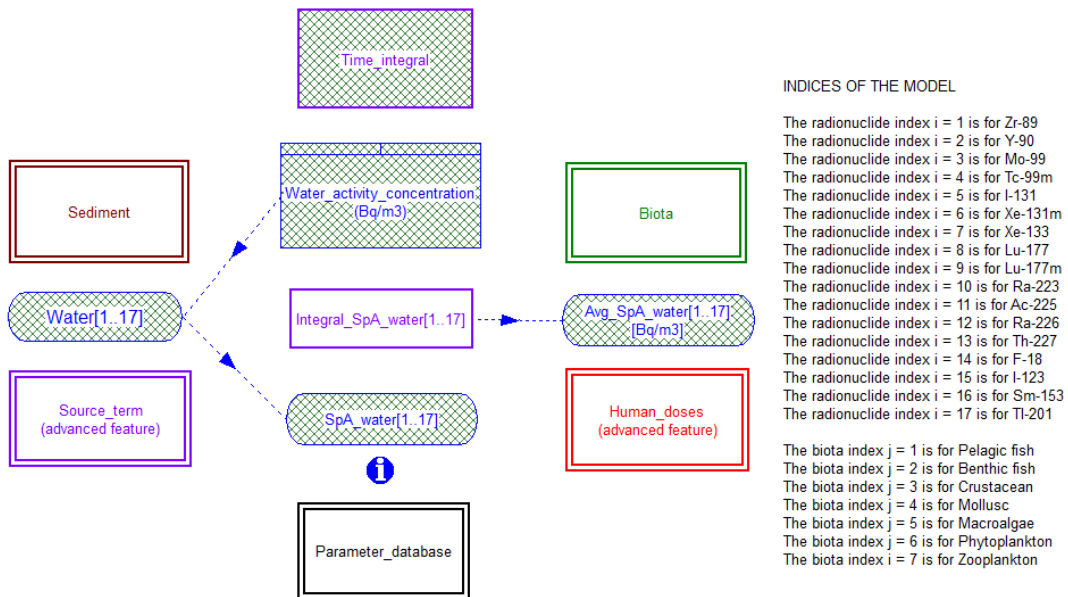
Figure 3: Upper level representation of the new version of D-DAT for freshwater in ModelMaker 4, showing integrating compartments (rectangles), embedded sub-models (double rectangles), variables (rounded rectangles) and influences (dotted arrows)
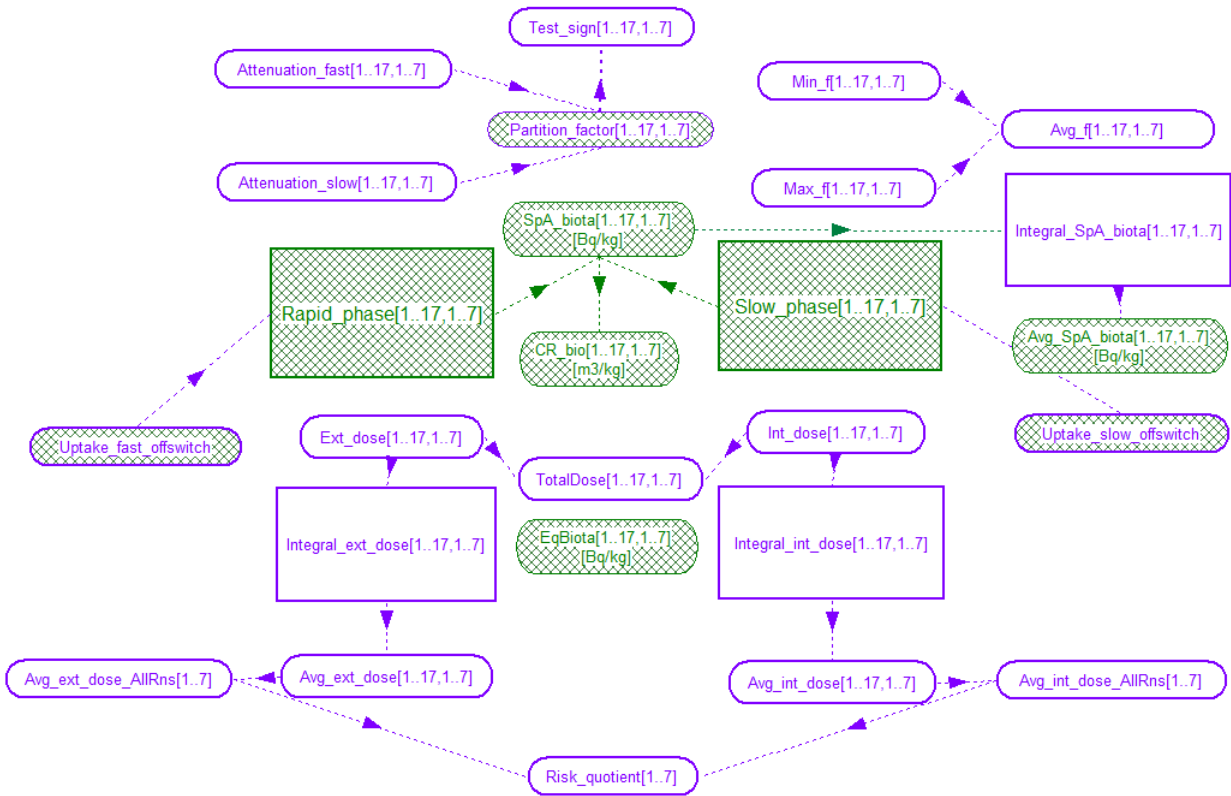
Figure 4: Wildlife calculation module for D-DAT version 5.1, showing integrating compartments (rectangles), variables (rounded rectangles) and influences (dotted arrows)
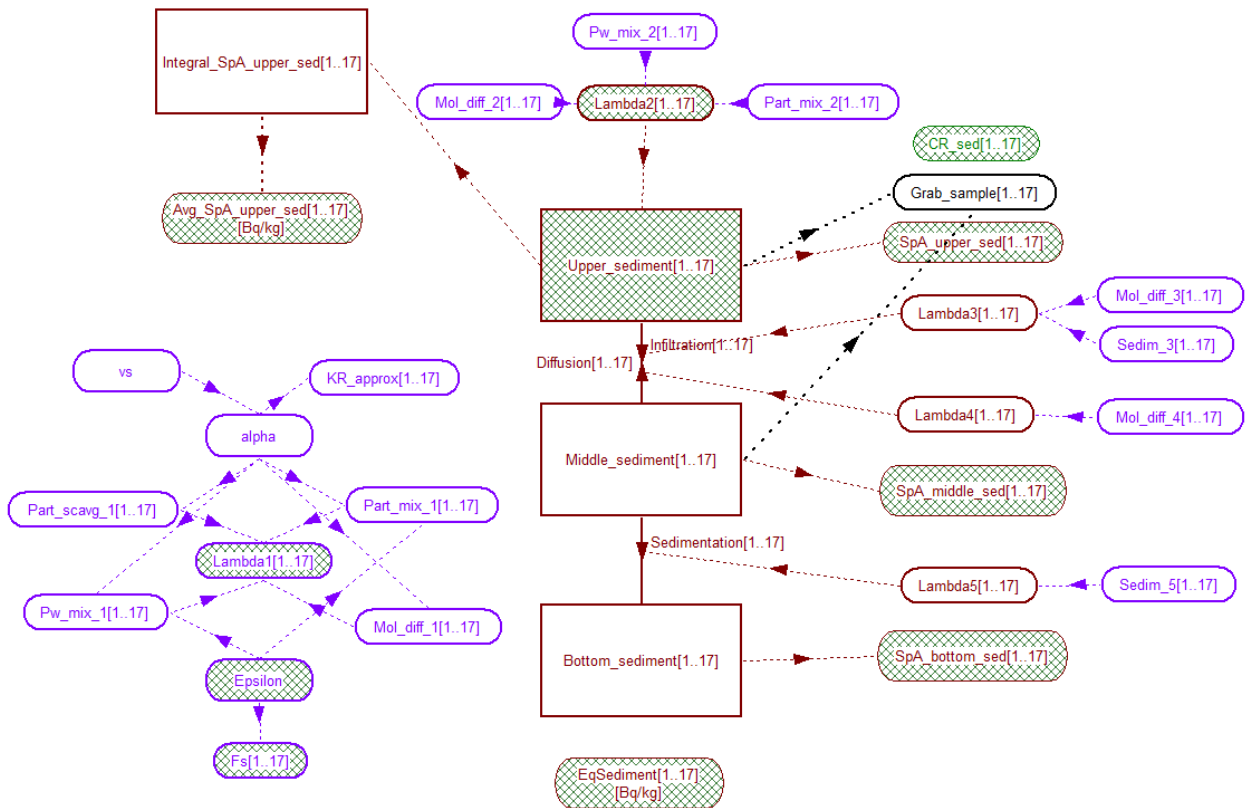
Figure 5: Sediment calculation module for D-DAT version 5.1, showing integrating compartments (rectangles), variables (rounded rectangles), flows (solid arrows) and influences (dotted arrows)
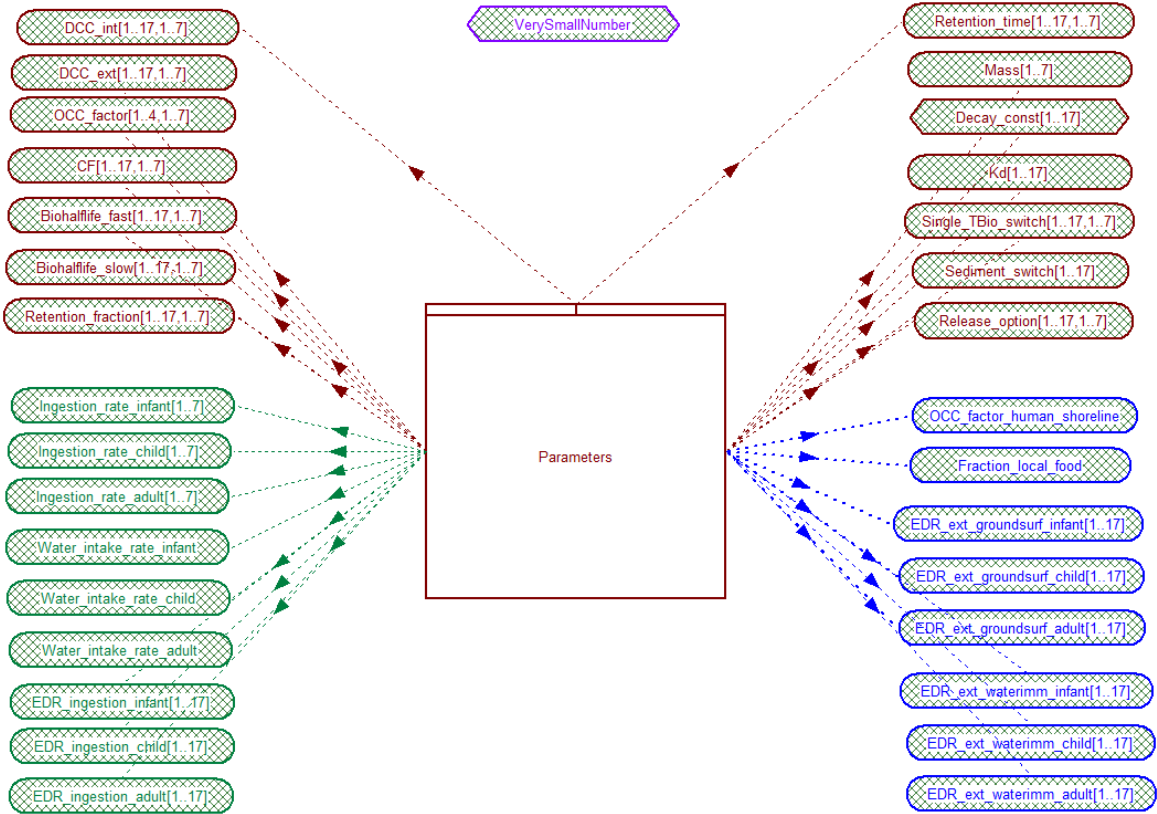
Figure 6: Parameter readout module for D-DAT version 5.1, the embedded lookout table, the read variables (rounded rectangles), definitions (hexagonal rectangle) and influences (dotted arrows)
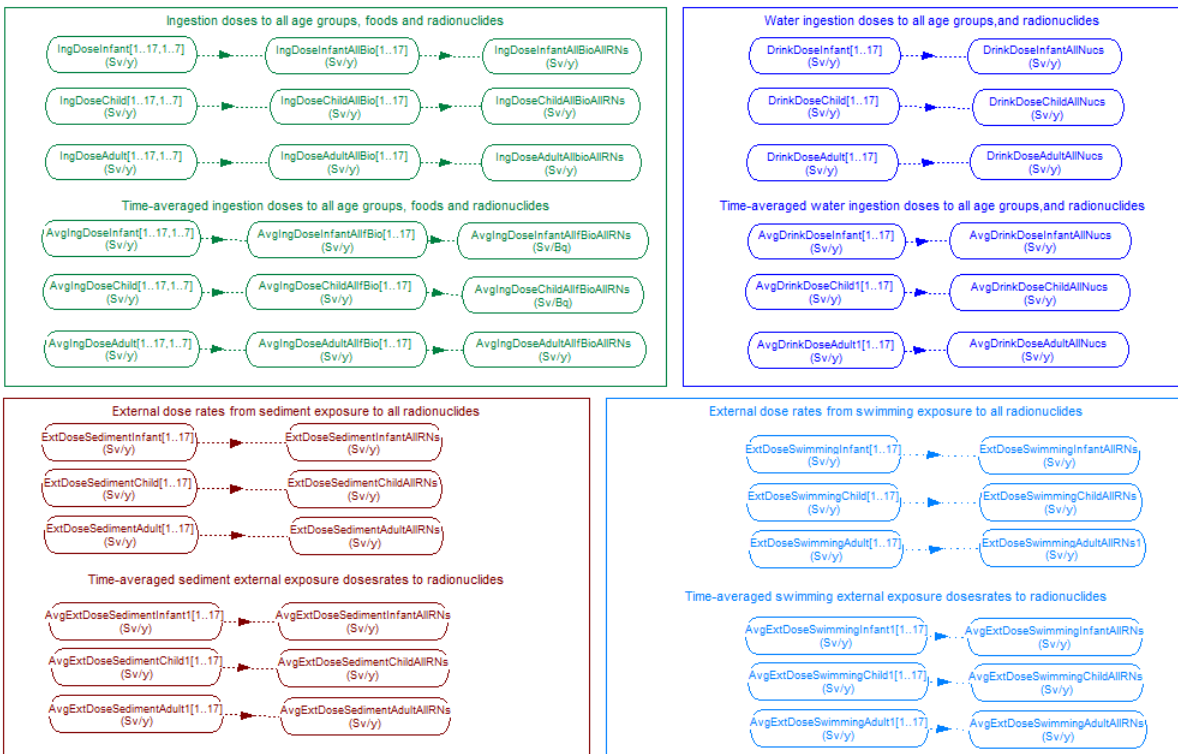
Figure 7: Human dose post-processor module for D-DAT version 5.1 with its read variables (rounded rectangles) and influences (dotted arrows)

The next improvement to the model was the introduction of a human dosimetry post-processing module, as shown in Figure 7. This module is capable of calculating: (a) time-dependent aquatic food ingestion doses, and associated time-averaged annual ingestion doses to all age groups, foods and radionuclides (the latter obtained by averaging the time-variable dose rates over a period of one year) (b) time-dependent and time-averaged annual water ingestion dose rates and (c) time-dependent, and also annually averaged, external dose rates from exposure to both sediment (riverbank) and water (swimming) exposure to all radionuclides.

Internal dose rates are calculated consistently with the conventional ICRP approach by multiplying the activity concentration in the wildlife used as food (Bq kg^{-1}) per the ingestion rate (kg y^{-1}), the dose per unit via intake via ingestion (Sv Bq^{-1}) from ICRP Publications 72 and 119 (ICRP, 1996, 2012) and the fraction of food that is obtained locally.

To calculate external exposures, the model uses the committed effective doses to 70 years of age per unit time and deposited activity of radionuclide on the shoreline in Sv Bq^{-1} s^{-1} m^2 (Eckerman and Ryman, 1993), maximally assumed to be as contaminated as sediment, so as to estimate doses for exposure to shoreline to members of the public. We deduced the modelled activity per unit area of shoreline soil (Bq m^{-2}) by multiplying the activity concentration by a 0.3 m active depth of contaminated soil, and this is in turn multiplied by the external dose coefficient and per the number of seconds in a year, with further application of a factor of 0.5 to account for the geometry of the source/target distribution on a marine shoreline and application of the occupancy factor, giving the external exposure dose rate.

The model uses an average individual shore occupancy rate of around 500 h per year (occupancy fraction of 5.7×10^{-2}), deemed to be sufficiently conservative. Any additional dose from irradiation of the skin due to direct contact with sediment is not included in the methodology because it is deemed not a major contributor to the overall doses.

The above extensions to the model required the addition of a new data block in the model parameter database, containing the aforementioned information: human food ingestion and water drinking rates for infant, child and adult, occupancy factor for external exposure to shoreline sediments, fraction of locally produced food, internal dose coefficients for ingestion and external dose coefficient for ground surface and water immersion.

Finally, the model was verified to check that all equations are correct. In particular, the complex input data structure shown in Fig. 6 was scrutinised to ensure that the input parameters are read correctly, and the integration algorithm was optimised, given the large number of data points of the input file provided by the hydrological simulations, which give a full year of water activity concentration data at 10-minute intervals. In the end, the Euler solving method was selected, with a random seed of one and running with a fixed step of 52555 user-defined output points (the number of output points in the Euler solver should match the data points in the input file).

5   Excel dose calculator for waste treatment plant workers, sewer maintenance workers and the public

The main route of hospital-released radionuclides to environment is from hospital to waste water treatment plants (WWTPs). The starting point for our estimation is the UK NRPB methodology for the radiological assessment of liquid pharmaceutical discharges in sewers (McDonnell, 2004; Titley et al., 2000), which has now been developed into the full-blown IRAT-2 approach (https://www.gov.uk/government/publications/initial-radiological-assessment-methodology). We used a highly modified and simplified approach adapted to suit the methodological needs of the Belgian situation, and we implemented the resulting equations in an Excel calculator to perform dose screening to workers and the public drinking the water and eating from the terrestrial foodchain, based on monthly concentration averages.

Unlike our model D-DAT for wildlife, these calculations are based on the assumption of steady state conditions, where discharges are assumed to take place at a uniform rate and there is little change in the flow rates down stream of the discharge point. This is because there is no simple equivalent of the D-DAT model in the form of a tool to calculate dynamically doses from short-lived radionuclides to humans. This would involve use of complex pharmacokinetic models, with an inevitable lack of associated parameter data for the radionuclides involved. In general, complex models comprise large number of parameters and variables often difficult to obtain. Therefore, it is important to simplify the model structure. Our chosen approach is considered appropriate for screening assessments because it is simple to use, requires relatively few parameters and is adequately conservative, even in the case of a single short release if the nominal average release rate is used in the dose calculations.

The calculator includes the following radionuclides: ^{18}F, ^{89}Zr, ^{90}Y, ^{99}Mo, ^{99m}Tc, ^{123}I, ^{131}I, ^{131m}Xe, ^{133}Xe, ^{153}Sm, ^{177}Lu, ^{177m}Lu, ^{201}Tl, ^{223}Ra, ^{225}Ac, ^{226}Ra and ^{227}Th. However, we used only ^{18}F, ^{123}I, ^{131}I, ^{153}Sm, ^{99m}Tc and ^{201}Tl as these are the only radionuclides for which we have activity concentrations as supplied to us by the authorities, who used automatic underwater measuring probes for measuring radioactivity (gamma spectrometry) in water treatment plants. Using as input annual discharges (calculated as average annual concentration in Bq m^{-3} multiplied by the flow rate in m^3 y^{-1}), this simple model calculates activity concentrations in the different waste streams at the WWTP; namely, for the WWTP effluent, for the case of a blocked sewer (which is a scenario of sewer maintenance close to or on the discharge site that would give the highest predicted dose) and for sludge, deriving doses to general and maintenance WWTP workers. This tool also calculates dose rates for the most exposed members of the public: consumers of locally caught fish, external exposure from frequenting the riverbank, direct drinking of river water, abstraction of river water for irrigation or drinking water and use of sludge for agricultural processes. However, it does so assuming average concentrations in water, thereby making a conservative estimation, whereas the D-DAT model is used to make a more detailed, dynamic calculation of doses to public and the environment – so exposes to the public can in effect be compared for a range of modelling assumptions.

5.1 Dosimetry tool description

The tool has the following calculation worksheets General assessment Parameters, Basic Radionuclide Data, Source Term Fractions, Calculation of dose rates and additional worksheets for Transfer factors, Dose factors and statement of assumptions.

The General Assessment Parameters worksheet, shown in Fig. 8, contains the required parameter data for the assessment: Disposal Pathway Parameters, Data for assessment of exposure of sewer workers, Data used for terrestrial food chain calculations, Data used for soil hydrology calculations and Habit data and other parameters for public exposure. Element independent parameters where chosen specific for the Belgian dataset from the Category A Waste Disposal project (Sweeck, 2018) or (when not available) literature values (McDonnell, 2004; Titley et al., 2000) or plain expert judgement.

The Basic Radionuclide Data parameters worksheet, shown in Fig. 9, contains radionuclide half-lives, external dose coefficients for ground surface and water immersion and internal dose coefficients for ingestion and inhalation for their stated lung classes. The key objective is the calculation of doses to workers and logically the focus is on the adults.

The Source Term Fractions worksheet, shown in Fig. 10, contains an estimation of the source term and fractions appearing in sewage, leading to estimation of the average radionuclide concentrations serving as source term for the different assessment locations of interest: Blocked Sewer scenario, WWTP water streams, WWTP sludge, the river ecosystem at the WWTP outlet and the use of river water for irrigation and drinking.

The Calculation of Dose Rates worksheet, shown in Fig. 11, is the main calculation block of the model, containing the equations to calculate dose rates to sewer maintenance workers, general workers at the sewage works, dose rates for the freshwater pathways and dose rates arising from use of river

water for irrigation of farmland and use of sewage sludge in agriculture (as detailed in Section 5.2). The last two worksheets, shown in Figs. 12 and 13, detail the transfer and dosimetry factors used in this model for information and data sourcing purposes.

Disposal Pathway Parameters

Parameter	Value	Units	Comment
Volume of liquid at site outfall blockage	1	m^3	NRPB report data typical of a UK sewer
Flow rate through sewer works	0.011574074	m^3 s^{-1}	
	1000	m^3 day^{-1}	NRPB report data typical of a UK sewer
Annual rate of sludge production to incoming sewage	0.02739726	Unitless	
Flow rate in river (1, fish and external pathways)	1.024702021	m^3 s^{-1}	Data from Molse Nete (Fabricio model calculations)
Flow rate in river (2, irrigation)	1.024702021	m^3 s^{-1}	Data from Molse Nete
Flow rate in river (3, public drinking water supply)	1.024702021	m^3 s^{-1}	Data from Molse Nete
Suspended sediment in river	4.00E-05	tonne m^{-3}	Data from Molse Nete
	4.00E-02	kg m^{-3}	
Average dry weather flow	1	ML day^{-1}	NRPB report data typical of a UK sewer
Annual Total volume of sludge	10000	m^3	NRPB report data typical of a UK sewer

Colour code

	Data needs to be input
	Data calculated by the tool

Data for assessment of exposure of sewer workers

Parameter	Blocked Sewer	Sewage Works	Units	Comment
Breathing Rate	1.69	1.69	m^3 h^{-1}	Data from Category A Waste Disposal project
Ingestion Rate	2.00E-05	2.00E-05	kg h^{-1}	Data from Category A Waste Disposal project
Average airborne particle concentration	2.30E-07	1.30E-06	kg m^{-3}	Data from Category A Waste Disposal project
Occupancy	2	1000	h y^{-1}	Conservative estimated occupancy in the vicinity of sludge presses by Titley et al (NRPBW63 report)
Ingested sewage	4.00E-05	2.00E-02	kg y^{-1}	
Inhaled sewage	7.77E-07	2.20E-03	kg y^{-1}	

Data used for terrestrial foodchain calculations

Parameter	Category	Value	Units	Comment
Irrigation by river water (unfiltered)		200	litres/m^2 per year	Data from Cat A project, data consumption rates for adult
Application rate of sewage sludge to farmland		8	kg/m2 per year	NRPB report data typical of a UK sewer
Food Consumption rates	Milk	75.1	L y^{-1}	Belgian food consumption rates for adult
	Beef	18.2	kg y^{-1}	Belgian food consumption rates for adult
	Sheep meat	3.6	kg y^{-1}	Belgian food consumption rates for adult
	Green Vegtables	45.2	kg y^{-1}	Belgian food consumption rates for adult
	Root vegtables	117.2	kg y^{-1}	Belgian food consumption rates for adult
Application rate of sewage sludge to farmland		8	kg m^{-2} per year	NRPB report data typical of a UK sewer

Data used for soil hydrology calculations

Parameter	Category	Value	Units	Comment
Volumetric water content		0.32	Unitless	Data from Category A Waste Disposal project
Soil bulk density		1350	kg m^{-3}	Data from Category A Waste Disposal project
Soil particle density		2650	kg m^{-3}	Density of quartz
Soil porosity		4.91E-01	Unitless	
Water density		1.00E+03	kg m^{-3}	Common knowledge
Active soil root depth		0.3	m	Data from Category A Waste Disposal project
Active depth in WWTP		0.05	m	To be confirmed

Habit data and other parameters for public exposure

Parameter	Value	Units	Comment
Drinking water consumption	0.4386	m^3 y^{-1}	Belgian food consumption rates for adult
Intakes of unfiltered river water	0.000731	m^3 y^{-1}	UK data scaled down to Belgian water consumption
Freshwater Fish consumption	6.5	kg y^{-1}	Belgian food consumption rates for adult
Riverbank Occupancy	500	h y^{-1}	Data from Category A Waste Disposal project
Years in an hour	0.000114077	y h^{-1}	General knowledge
Seconds in a year	3.16E+07	s y^{-1}	General knowledge

Figure 8: Tool for assessment of human dose rates. General assessment parameters

Basic Radionuclide Data

Radionuclide	Half-Life (days)	External Dose Coefficients (adults) Ground surface (Sv Bq^{-1} s^{-1} m^2)	External Dose Coefficients (adults) Water immersion (Sv Bq^{-1} s^{-1} m^3)	Internal Dose Coefficients (adults) Ingestion Sv/Bq	Internal Dose Coefficients (adults) Inhalation Sv/Bq	Lung Class	Concentration Factors (m^3/kg for Kd and kg/kg for biota) Freshwater Sediment (Kd)	Freshwater Fish	Green vegetables	Root vegetables	Food concentration from deposited activity ratio (Bq/kg for 1 Bq/m^2 per second) Green Vegtables	Root Vegtables
^{89}Zr	3.27E+00	7.35E-16	1.1E-16	7.90E-10	2.90E-10	F	1.71E+02	1.26E+00	4.00E-03	4.00E-03	4.02E+00	4.02E+00
^{90}Y	2.67E+00	1.47E-16	9.48E-19	2.70E-09	1.40E-09	M	4.00E+00	7.90E-02	2.00E-03	2.00E-03	1.64E+00	1.64E+00
^{99}Mo	2.75E+00	1.42E-16	1.4E-17	6.00E-10	2.20E-10	F	2.59E-02	9.90E-02	5.10E-01	3.20E-01	4.28E+02	2.68E+02
^{99m}Tc	2.51E-01	7.06E-17	9.86E-18	2.20E-11	1.20E-11	F	2.59E-02	9.90E-02	1.80E+02	4.60E+01	1.38E+04	3.52E+03
^{131}I	8.04E+00	2.44E-16	3.36E-17	2.20E-08	7.40E-09	F	1.14E+00	3.10E-01	3.00E-01	3.00E-01	7.42E+02	7.42E+02
^{131m}Xe	1.19E+01	4.14E-18	6.24E-19	0.00E+00	3.20E-11	Inert gas	0.00E+00	0.00E+00	0.00E+00	0.00E+00	0.00E+00	0.00E+00
^{133}Xe	5.25E+00	2.09E-17	2.44E-18	0.00E+00	1.20E-10	Inert gas	0.00E+00	0.00E+00	0.00E+00	0.00E+00	0.00E+00	0.00E+00
^{177}Lu	6.71E+00	2.24E-17	2.78E-18	5.30E-10	1.10E-09	M	2.85E+02	6.17E-02	6.00E-03	6.00E-03	1.24E+01	1.24E+01
^{177m}Lu	1.61E+02	5.80E-16	8.16E-17	1.70E-09	1.30E-08	M	2.85E+02	6.17E-02	6.00E-03	6.00E-03	2.97E+02	2.97E+02
^{223}Ra	1.14E+01	7.86E-17	1.09E-17	1.00E-07	7.40E-06	M	8.47E+00	1.04E+00	2.80E-02	7.00E-02	9.85E+01	2.46E+02
^{225}Ac	1.00E+01	7.71E-18	1.06E-18	2.40E-08	8.80E-07	F	2.00E+04	1.13E+00	2.80E-02	7.00E-02	8.62E+01	2.15E+02
^{226}Ra	5.84E+05	4.09E-18	5.87E-19	2.80E-07	3.50E-06	M	8.47E+00	1.04E+00	2.80E-02	7.00E-02	5.04E+06	1.26E+07
^{227}Th	1.87E+01	7.00E-17	9.99E-18	8.80E-09	8.50E-06	M	2.68E+02	7.17E-01	2.00E-02	2.00E-02	1.15E+02	1.15E+02
^{18}F	7.62E-02	6.49E-16	8.93E-17	4.90E-11	5.90E-11	S	1.00E-03	1.02E+00	2.60E-01	1.20E-01	4.93E+02	2.28E+02
^{123}I	5.50E-01	8.74E-17	1.24E-17	2.10E-10	7.40E-11	F	1.14E+00	3.10E-01	3.00E-01	3.00E-01	5.08E+01	5.08E+01
^{153}Sm	1.95E+00	3.98E-17	3.77E-18	7.40E-10	6.30E-10	M	2.85E+02	6.17E-02	6.00E-03	6.00E-03	3.59E+00	3.59E+00
^{201}Tl	3.04E+00	4.68E-17	5.91E-18	9.50E-11	4.40E-11	F	1.70E+00	3.99E+00	8.00E-02	1.50E-02	7.49E+01	1.41E+01

Note: 1 Bq tonne per Bq/m^3 = 1 L/kg   Note: Cl analog for F, Tc for Mo and Eu for Sm, Lu

Figure 9: Tool for assessment of human dose rates – Basic radionuclide input data

Source term and fractions appearing in sewage

Radionuclide	Half-Life (days)	Mean Monthly Discharge	Mean Annual Discharge	Average Discharge Rate	Fractions in Sewage Materials		
					Reaching Sewage Works	Removal Efficiency for	In sludge at STP
		Bq	Bq	Bq/s			
^{89}Zr	3.27E+00		0.00E+00	0.00E+00	1		
^{90}Y	2.67E+00		0.00E+00	0.00E+00	1		
^{99}Mo	2.75E+00		0.00E+00	0.00E+00	1		
^{99m}Tc	2.51E-01	6.92E+10	8.30E+11	2.63E+04	1	0.9	0
^{131}I	8.04E+00	5.07E+08	6.09E+09	1.93E+02	1	0.2	0.05
^{131m}Xe	1.19E+01		0.00E+00	0.00E+00	1	0	0
^{133}Xe	5.25E+00		0.00E+00	0.00E+00	1	0	0
^{177}Lu	6.71E+00		0.00E+00	0.00E+00	1		
^{177m}Lu	1.61E+02		0.00E+00	0.00E+00	1		
^{223}Ra	1.14E+01		0.00E+00	0.00E+00	1		
^{225}Ac	1.00E+01		0.00E+00	0.00E+00	1		
^{226}Ra	5.84E+05		0.00E+00	0.00E+00	1		
^{227}Th	1.87E+01		0.00E+00	0.00E+00	1		
^{18}F	7.62E-02	1.15E+09	1.38E+10	4.38E+02	1	0.9	0
^{123}I	5.50E-01	1.10E+09	1.32E+10	4.17E+02	1	0.9	0
^{153}Sm	1.95E+00	1.14E+08	1.36E+09	4.32E+01	1	0.8	0.01
^{201}Tl	3.04E+00	2.10E+11	2.52E+12	7.98E+04	1	0.8	0.01

Average Radionuclide Concentrations

Radionuclide	Activity in blocked drain as % of monthly limit	Average Concentrations (Bq/m^3)					
		Blocked Sewer	In liquid at WWTP	In sludge at STP	River ecosystem	River Irrigation	River Drinking
^{89}Zr	1	0.0E+00	0.0E+00	0.0E+00	0.0E+00	0.0E+00	0.0E+00
^{90}Y	1	0.0E+00	0.0E+00	0.0E+00	0.0E+00	0.0E+00	0.0E+00
^{99}Mo	1	0.0E+00	0.0E+00	0.0E+00	0.0E+00	0.0E+00	0.0E+00
^{99m}Tc	1	8.3E+06	2.3E+06	0.0E+00	2.6E+03	2.6E+03	2.6E+03
^{131}I	1	2.0E+06	1.7E+04	3.0E+04	1.5E+02	1.5E+02	1.5E+02
^{131m}Xe	1	0.0E+00	0.0E+00	0.0E+00	0.0E+00	0.0E+00	0.0E+00
^{133}Xe	1	0.0E+00	0.0E+00	0.0E+00	0.0E+00	0.0E+00	0.0E+00
^{177}Lu	1	0.0E+00	0.0E+00	0.0E+00	0.0E+00	0.0E+00	0.0E+00
^{177m}Lu	1	0.0E+00	0.0E+00	0.0E+00	0.0E+00	0.0E+00	0.0E+00
^{223}Ra	1	0.0E+00	0.0E+00	0.0E+00	0.0E+00	0.0E+00	0.0E+00
^{225}Ac	1	0.0E+00	0.0E+00	0.0E+00	0.0E+00	0.0E+00	0.0E+00
^{226}Ra	1	0.0E+00	0.0E+00	0.0E+00	0.0E+00	0.0E+00	0.0E+00
^{227}Th	1	0.0E+00	0.0E+00	0.0E+00	0.0E+00	0.0E+00	0.0E+00
^{18}F	1	4.2E+04	3.8E+04	0.0E+00	4.3E+01	4.3E+01	4.3E+01
^{123}I	1	2.9E+05	3.6E+04	0.0E+00	4.1E+01	4.1E+01	4.1E+01
^{153}Sm	1	1.1E+05	3.7E+03	1.4E+03	8.4E+00	8.4E+00	8.4E+00
^{201}Tl	1	3.1E+08	6.9E+06	2.5E+06	1.6E+04	1.6E+04	1.6E+04

Figure 10: Tool for assessment of human dose rates – Source term fractions

Doses to sewer maintenance workers

Radionuclide	Ingestion $Sv\ y^{-1}$	Inhalation $Sv\ y^{-1}$	External Gamma $Sv\ y^{-1}$	Totals $Sv\ y^{-1}$
^{89}Zr	0.0E+00	0.0E+00	0.0E+00	0.0E+00
^{90}Y	0.0E+00	0.0E+00	0.0E+00	0.0E+00
^{99}Mo	0.0E+00	0.0E+00	0.0E+00	0.0E+00
^{99m}Tc	7.3E-12	7.8E-14	2.1E-07	2.1E-07
^{131}I	1.7E-09	1.1E-11	1.7E-07	1.7E-07
^{131m}Xe	0.0E+00	0.0E+00	0.0E+00	0.0E+00
^{133}Xe	0.0E+00	0.0E+00	0.0E+00	0.0E+00
^{177}Lu	0.0E+00	0.0E+00	0.0E+00	0.0E+00
^{177m}Lu	0.0E+00	0.0E+00	0.0E+00	0.0E+00
^{223}Ra	0.0E+00	0.0E+00	0.0E+00	0.0E+00
^{225}Ac	0.0E+00	0.0E+00	0.0E+00	0.0E+00
^{226}Ra	0.0E+00	0.0E+00	0.0E+00	0.0E+00
^{227}Th	0.0E+00	0.0E+00	0.0E+00	0.0E+00
^{18}F	8.3E-14	1.9E-15	9.9E-09	9.9E-09
^{123}I	2.4E-12	1.7E-14	9.1E-09	9.1E-09
^{153}Sm	3.1E-12	5.2E-14	1.5E-09	1.5E-09
^{201}Tl	1.2E-09	1.1E-11	5.2E-06	5.2E-06
Totals	2.9E-09	2.2E-11	5.6E-06	5.6E-06

Doses to workers at the WWTP

Radionuclide	Ingestion $Sv\ y^{-1}$	Inhalation $Sv\ y^{-1}$	External Gamma $Sv\ y^{-1}$	Totals $Sv\ y^{-1}$
^{89}Zr	0.0E+00	0.0E+00	0.0E+00	0.0E+00
^{90}Y	0.0E+00	0.0E+00	0.0E+00	0.0E+00
^{99}Mo	0.0E+00	0.0E+00	0.0E+00	0.0E+00
^{99m}Tc	5.0E-10	3.0E-11	1.4E-05	1.4E-05
^{131}I	1.0E-08	3.8E-10	1.0E-06	1.0E-06
^{131m}Xe	0.0E+00	0.0E+00	0.0E+00	0.0E+00
^{133}Xe	0.0E+00	0.0E+00	0.0E+00	0.0E+00
^{177}Lu	0.0E+00	0.0E+00	0.0E+00	0.0E+00
^{177m}Lu	0.0E+00	0.0E+00	0.0E+00	0.0E+00
^{223}Ra	0.0E+00	0.0E+00	0.0E+00	0.0E+00
^{225}Ac	0.0E+00	0.0E+00	0.0E+00	0.0E+00
^{226}Ra	0.0E+00	0.0E+00	0.0E+00	0.0E+00
^{227}Th	0.0E+00	0.0E+00	0.0E+00	0.0E+00
^{18}F	1.9E-11	2.5E-12	2.2E-06	2.2E-06
^{123}I	7.6E-11	2.9E-12	2.8E-07	2.8E-07
^{153}Sm	3.8E-11	3.5E-12	1.8E-08	1.8E-08
^{201}Tl	8.9E-09	4.6E-10	4.0E-05	4.0E-05
Totals	2.0E-08	8.8E-10	5.8E-05	5.8E-05

Doses for freshwater pathways

Radionuclide	Input rate to river $MBq\ y^{-1}$	External gamma (riverbank occupancy) $Sv\ y^{-1}$	Fish $Sv\ y^{-1}$	Drinking water $Sv\ y^{-1}$	Unfiltered river water $Sv\ y^{-1}$
^{89}Zr	0.0E+00	0.0E+00	0.0E+00	0.0E+00	0.0E+00
^{90}Y	0.0E+00	0.0E+00	0.0E+00	0.0E+00	0.0E+00
^{99}Mo	0.0E+00	0.0E+00	0.0E+00	0.0E+00	0.0E+00
^{99m}Tc	8.3E+04	4.4E-07	3.6E-11	2.5E-08	4.1E-11
^{131}I	4.9E+03	3.9E-06	6.4E-09	1.4E-06	2.4E-09
^{131m}Xe	0.0E+00	0.0E+00	0.0E+00	0.0E+00	0.0E+00
^{133}Xe	0.0E+00	0.0E+00	0.0E+00	0.0E+00	0.0E+00
^{177}Lu	0.0E+00	0.0E+00	0.0E+00	0.0E+00	0.0E+00
^{177m}Lu	0.0E+00	0.0E+00	0.0E+00	0.0E+00	0.0E+00
^{223}Ra	0.0E+00	0.0E+00	0.0E+00	0.0E+00	0.0E+00
^{225}Ac	0.0E+00	0.0E+00	0.0E+00	0.0E+00	0.0E+00
^{226}Ra	0.0E+00	0.0E+00	0.0E+00	0.0E+00	0.0E+00
^{227}Th	0.0E+00	0.0E+00	0.0E+00	0.0E+00	0.0E+00
^{18}F	1.4E+03	2.6E-09	1.4E-11	9.2E-10	1.5E-12
^{123}I	1.3E+03	3.8E-07	1.6E-11	3.6E-09	6.2E-12
^{153}Sm	2.7E+02	8.9E-06	2.0E-13	2.2E-10	4.6E-12
^{201}Tl	5.0E+05	1.2E-04	3.6E-08	6.1E-07	1.1E-09
Totals	5.9E+05	1.3E-04	4.2E-08	2.0E-06	3.6E-09

Assessment of use of sewage sludge in agriculture

Radionuclide	Concentration in sludge Bq/kg	Conc. in soil per unit $Bq\ kg^{-1}$ per $Bq\ m^{-2}\ y^{-1}$	Dose for given Sv/y
^{89}Zr	0.0E+00	3.2E-05	0.0E+00
^{90}Y	0.0E+00	2.6E-05	0.0E+00
^{99}Mo	0.0E+00	2.7E-05	0.0E+00
^{99m}Tc	0.0E+00	2.4E-06	0.0E+00
^{131}I	3.0E+01	7.8E-05	1.0E-08
^{131m}Xe	0.0E+00	1.2E-04	0.0E+00
^{133}Xe	0.0E+00	5.1E-05	0.0E+00
^{177}Lu	0.0E+00	6.5E-05	0.0E+00
^{177m}Lu	0.0E+00	1.6E-03	0.0E+00
^{223}Ra	0.0E+00	1.1E-04	0.0E+00
^{225}Ac	0.0E+00	9.8E-05	0.0E+00
^{226}Ra	0.0E+00	5.7E+00	0.0E+00
^{227}Th	0.0E+00	1.8E-04	0.0E+00
^{18}F	0.0E+00	7.4E-07	0.0E+00
^{123}I	0.0E+00	5.4E-06	0.0E+00
^{153}Sm	1.4E+00	1.9E-05	1.8E-11
^{201}Tl	2.5E+03	3.0E-05	6.1E-08
Totals	2.5E+03	5.7E+00	7.1E-08

Use of river water for irrigation of farmland

Radionuclide	Application rate $Bq\ m^{-2}\ s^{-1}$	Food Concentrations Green Vegtables $Bq\ kg^{-1}$	Root Vegtables $Bq\ kg^{-1}$	Doses for each foodstuff Green Vegtables $Sv\ y^{-1}$	Root Vegtables $Sv\ y^{-1}$	Total $Sv\ y^{-1}$
^{89}Zr	0.0E+00	0.0E+00	0.0E+00	0.0E+00	0.0E+00	0.0E+00
^{90}Y	0.0E+00	0.0E+00	0.0E+00	0.0E+00	0.0E+00	0.0E+00
^{99}Mo	0.0E+00	0.0E+00	0.0E+00	0.0E+00	0.0E+00	0.0E+00
^{99m}Tc	1.6E-05	2.2E-01	5.7E-02	2.2E-10	1.5E-10	3.7E-10
^{131}I	9.5E-07	7.1E-04	7.1E-04	7.0E-10	1.8E-09	2.5E-09
^{131m}Xe	0.0E+00	0.0E+00	0.0E+00	0.0E+00	0.0E+00	0.0E+00
^{133}Xe	0.0E+00	0.0E+00	0.0E+00	0.0E+00	0.0E+00	0.0E+00
^{177}Lu	0.0E+00	0.0E+00	0.0E+00	0.0E+00	0.0E+00	0.0E+00
^{177m}Lu	0.0E+00	0.0E+00	0.0E+00	0.0E+00	0.0E+00	0.0E+00
^{223}Ra	0.0E+00	0.0E+00	0.0E+00	0.0E+00	0.0E+00	0.0E+00
^{225}Ac	0.0E+00	0.0E+00	0.0E+00	0.0E+00	0.0E+00	0.0E+00
^{226}Ra	0.0E+00	0.0E+00	0.0E+00	0.0E+00	0.0E+00	0.0E+00
^{227}Th	0.0E+00	0.0E+00	0.0E+00	0.0E+00	0.0E+00	0.0E+00
^{18}F	2.7E-07	1.3E-04	6.2E-05	3.0E-13	3.5E-13	6.5E-13
^{123}I	2.6E-07	1.3E-05	1.3E-05	1.2E-13	3.2E-13	4.5E-13
^{153}Sm	5.3E-08	1.9E-07	1.9E-07	6.4E-15	1.7E-14	2.3E-14
^{201}Tl	9.9E-05	7.4E-03	1.4E-03	3.2E-11	1.5E-11	4.7E-11
Totals	1.2E-04	2.3E-01	5.9E-02	9.6E-10	2.0E-09	2.9E-09

Figure 11: Tool for assessment of human dose rates - Dose rate results

Transfer factors for foodstuffs

Radionuclide	Leafy vegetables	Root crops	Analogue used
^{89}Zr	4.00E-03	4.00E-03	IAEA TRS 472
^{90}Y	2.00E-03	2.00E-03	IAEA TRS 472
^{99}Mo	5.10E-01	3.20E-01	IAEA TRS 472
^{99m}Tc	1.80E+02	4.60E+01	IAEA TRS 472
^{131}I	3.00E-01	3.00E-01	Use Te as analogue
^{131m}Xe	0.00E+00	0.00E+00	IAEA TRS 472
^{133}Xe	0.00E+00	0.00E+00	IAEA TRS 472
^{177}Lu	6.00E-03	6.00E-03	Use Ce as analogue
^{177m}Lu	6.00E-03	6.00E-03	Use Ce as analogue
^{223}Ra	2.80E-02	7.00E-02	IAEA TRS 472
^{225}Ac	2.80E-02	7.00E-02	Use Ra as analogue
^{226}Ra	2.80E-02	7.00E-02	IAEA TRS 472
^{227}Th	2.00E-02	2.00E-02	Assume roots same as greens
^{18}F	2.60E+01	1.20E+01	Using Cl as analogue
^{123}I	3.00E-01	3.00E-01	Use Te as analogue
^{153}Sm	6.00E-03	6.00E-03	Use Ce as analogue
^{201}Tl	8.00E-02	1.50E-02	Use Pb as analogue

Figure 12: Tool for assessment of human dose rates – Input data: transfer factors

Internal exposure via ingestion (Sv/Bq)

Radionuvclide	Halflife	Unit	Halflife	Unit	λ (d⁻¹)	1 year	5 years	10 years	15 years	Adult
^{89}Zr	7.84E+01	h	3.27E+00	d	2.12E-01	4.5E-09	2.5E-09	1.6E-09	9.9E-10	7.9E-10
^{90}Y	6.40E+01	h	2.67E+00	d	2.60E-01	2.0E-08	1.0E-08	5.9E-09	3.3E-09	2.7E-09
^{99}Mo	6.60E+01	h	2.75E+00	d	2.52E-01	3.5E-09	1.8E-09	1.1E-09	7.6E-10	6.0E-10
^{99m}Tc	6.02E+00	h	2.51E-01	d	2.76E+00	1.3E-10	7.2E-11	4.3E-11	2.8E-11	2.2E-11
^{131}I	8.04E+00	d	8.04E+00	d	8.62E-02	1.8E-07	1.0E-07	5.2E-08	3.4E-08	2.2E-08
^{131m}Xe	1.19E+01	d	1.19E+01	d	5.82E-02	0.0E+00	0.0E+00	0.0E+00	0.0E+00	0.0E+00
^{133}Xe	5.25E+00	d	5.25E+00	d	1.32E-01	0.0E+00	0.0E+00	0.0E+00	0.0E+00	0.0E+00
^{177}Lu	6.71E+00	d	6.71E+00	d	1.03E-01	3.9E-09	2.0E-09	1.2E-09	6.6E-10	5.3E-10
^{177m}Lu	1.61E+02	d	1.61E+02	d	4.31E-03	1.1E-08	5.8E-09	3.6E-09	2.1E-09	1.7E-09
^{223}Ra	1.14E+01	d	1.14E+01	d	6.06E-02	1.1E-06	5.7E-07	4.5E-07	3.7E-07	1.0E-07
^{225}Ac	1.00E+01	d	1.00E+01	d	6.93E-02	1.8E-07	9.1E-08	5.4E-08	3.0E-08	2.4E-08
^{226}Ra	1.60E+03	y	5.84E+05	d	1.19E-06	9.6E-07	6.2E-07	8.0E-07	1.5E-06	2.8E-07
^{227}Th	1.87E+01	d	1.87E+01	d	3.70E-02	7.0E-08	3.6E-08	2.3E-08	1.5E-08	8.8E-09
^{18}F	1.10E+02	m	7.62E-02	d	9.09E+00	3.0E-10	1.5E-10	9.1E-11	6.2E-11	4.9E-11
^{123}I	1.32E+01	h	5.50E-01	d	1.26E+00	1.9E-09	1.1E-09	4.9E-10	3.3E-10	2.1E-10
^{153}Sm	4.67E+01	h	1.95E+00	d	3.56E-01	5.4E-09	2.7E-09	1.6E-09	9.2E-10	7.4E-10
^{201}Tl	3.04E+00	d	3.04E+00	d	2.28E-01	5.5E-10	2.9E-10	1.8E-10	1.2E-10	9.5E-11

Internal exposure via inhalation (Sv/Bq) for members of the public

Radionuvclide	Halflife	Unit	Halflife	Unit	λ (d⁻¹)	Lung class	DC	Lung class	DC	Lung class	DC	Inert gas	DC	Selection	
^{89}Zr	7.84E+01	h	3.27E+00	d	2.12E-01	F	2.90E-10	M	5.20E-10	S	5.50E-10	N		F	2.90E-10
^{90}Y	6.40E+01	h	2.67E+00	d	2.60E-01	F	NA	M	1.40E-09	S	1.50E-09	N		M	1.40E-09
^{99}Mo	6.60E+01	h	2.75E+00	d	2.52E-01	F	2.20E-10	M	8.90E-10	S	9.90E-10	N		F	2.20E-10
^{99m}Tc	6.02E+00	h	2.51E-01	d	2.76E+00	F	1.20E-11	M	1.90E-11	S	2.00E-11	N		F	1.20E-11
^{131}I	8.04E+00	d	8.04E+00	d	8.62E-02	F	7.40E-09	M	2.40E-09	S	1.60E-09	N		F	7.40E-09
^{131m}Xe	1.19E+01	d	1.19E+01	d	5.82E-02	F		M		S		Y	3.20E-11	IG	3.20E-11
^{133}Xe	5.25E+00	d	5.25E+00	d	1.32E-01	F		M		S		Y	1.20E-10	IG	1.20E-10
^{177}Lu	6.71E+00	d	6.71E+00	d	1.03E-01	F	NA	M	1.10E-09	S	1.20E-09	N		M	1.10E-09
^{177m}Lu	1.61E+02	d	1.61E+02	d	4.31E-03	F	NA	M	1.30E-08	S	1.60E-08	N		M	1.30E-08
^{223}Ra	1.14E+01	d	1.14E+01	d	6.06E-02	F	1.20E-07	M	7.40E-06	S	8.70E-06	N		M	7.40E-06
^{225}Ac	1.00E+01	d	1.00E+01	d	6.93E-02	F	8.80E-07	M	7.40E-06	S	8.50E-06	N		F	8.80E-07
^{226}Ra	1.60E+03	y	5.84E+05	d	1.19E-06	F	3.60E-07	M	3.50E-06	S	9.50E-06	N		M	3.50E-06
^{227}Th	1.87E+01	d	1.87E+01	d	3.70E-02	F	6.70E-07	M	8.50E-06	S	1.00E-05	N		M	8.50E-06
^{18}F	1.10E+02	m	7.62E-02	d	9.09E+00	F	2.80E-11	M	5.60E-11	S	5.90E-11	N		S	5.90E-11
^{123}I	1.32E+01	h	5.50E-01	d	1.26E+00	F	7.40E-11	M	6.40E-11	S	6.00E-11	N		F	7.40E-11
^{153}Sm	4.67E+01	h	1.95E+00	d	3.56E-01	F	NA	M	6.30E-10	S	NA	N		M	6.30E-10
^{201}Tl	3.04E+00	d	3.04E+00	d	2.28E-01	F	4.40E-11	M	NA	S	NA	N		F	4.40E-11

Select the lung class for the workers with the help of table E of the compendium. Workers are assumed to have higher breathing rates

External exposure for ground surface (Sv Bq⁻¹ s⁻¹ m²)

Radionuvclide	Newborn	1-yr-old	5-yr-old	10-yr-old	15-yr-old	Adult
^{89}Zr	9.43E-16	8.82E-16	8.63E-16	8.04E-16	7.51E-16	7.35E-16
^{90}Y	1.58E-16	1.54E-16	1.54E-16	1.50E-16	1.47E-16	1.47E-16
^{99}Mo	1.73E-16	1.64E-16	1.60E-16	1.52E-16	1.44E-16	1.42E-16
^{99m}Tc	9.66E-17	9.51E-17	8.08E-17	7.78E-17	7.18E-17	7.06E-17
^{131}I	3.23E-16	3.03E-16	2.83E-16	2.74E-16	2.50E-16	2.44E-16
^{131m}Xe	8.97E-18	7.12E-18	5.65E-18	5.24E-18	4.28E-18	4.14E-18
^{133}Xe	3.29E-17	2.90E-17	2.57E-17	2.44E-17	2.17E-17	2.09E-17
^{177}Lu	3.15E-17	2.91E-17	2.72E-17	2.63E-17	2.30E-17	2.24E-17
^{177m}Lu	8.00E-16	7.47E-16	6.87E-16	6.72E-16	5.94E-16	5.80E-16
^{223}Ra	1.09E-16	1.01E-16	9.31E-17	9.02E-17	8.08E-17	7.86E-17
^{225}Ac	1.09E-17	9.98E-18	9.13E-18	8.73E-18	7.95E-18	7.71E-18
^{226}Ra	5.76E-18	5.46E-18	4.94E-18	4.86E-18	4.17E-18	4.09E-18
^{227}Th	9.82E-17	9.07E-17	8.46E-17	8.31E-17	7.17E-17	7.00E-17
^{18}F	8.39E-16	7.90E-16	7.32E-16	7.02E-16	6.66E-16	6.49E-16
^{123}I	1.2E-16	1.2E-16	1.0E-16	9.9E-17	8.9E-17	8.7E-17
^{153}Sm	5.8E-17	5.0E-17	4.8E-17	4.5E-17	4.1E-17	4.0E-17
^{201}Tl	6.67E-17	6.39E-17	5.57E-17	5.57E-17	4.83E-17	4.68E-17

External exposure for water immersion (Sv Bq⁻¹ s⁻¹ m³)

Radionuvclide	Newborn	1-yr-old	5-yr-old	10-yr-old	15-yr-old	Adult
^{89}Zr	1.49E-16	1.38E-16	1.28E-16	1.25E-16	1.12E-16	1.10E-16
^{90}Y	1.10E-18	1.05E-18	1.01E-18	9.91E-19	9.54E-19	9.48E-19
^{99}Mo	1.93E-17	1.76E-17	1.63E-17	1.58E-17	1.42E-17	1.40E-17
^{99m}Tc	1.56E-17	1.36E-17	1.22E-17	1.13E-17	1.01E-17	9.86E-18
^{131}I	4.82E-17	4.35E-17	3.98E-17	3.83E-17	3.41E-17	3.36E-17
^{131m}Xe	1.30E-18	9.75E-19	8.39E-19	7.80E-19	6.47E-19	6.24E-19
^{133}Xe	4.54E-18	3.66E-18	2.91E-18	2.85E-18	2.55E-18	2.44E-18
^{177}Lu	4.37E-18	3.79E-18	3.35E-18	3.17E-18	2.83E-18	2.78E-18
^{177m}Lu	1.24E-16	1.09E-16	9.83E-17	9.37E-17	8.30E-17	8.16E-17
^{223}Ra	1.70E-17	1.48E-17	1.29E-17	1.24E-17	1.11E-17	1.09E-17
^{225}Ac	1.72E-18	1.48E-18	1.27E-18	1.20E-18	1.09E-18	1.06E-18
^{226}Ra	9.18E-19	7.98E-19	7.16E-19	6.78E-19	5.97E-19	5.87E-19
^{227}Th	1.54E-17	1.34E-17	1.20E-17	1.15E-17	1.02E-17	9.99E-18
^{18}F	1.24E-16	1.14E-16	1.05E-16	1.01E-16	9.07E-17	8.93E-17
^{123}I	1.96E-17	1.70E-17	1.54E-17	1.45E-17	1.27E-17	1.24E-17
^{153}Sm	6.75E-18	5.53E-18	4.60E-18	4.26E-18	3.92E-18	3.77E-18
^{201}Tl	1.03E-17	8.61E-18	7.03E-18	7.02E-18	6.14E-18	5.91E-18

Figure 13: Tool for assessment of human dose rates – Input data: dose factors

5.2 Equations used for dose calculation

5.2.1 Calculation of activity concentrations in blocked sewer and the river

The mean cumulative discharge over a month in Bq, A_M [Bq] is the main input to the model. We assume that 100% of the radionuclides discharged from the hospital reach the WWTP, which is a conservative assumption but one that allows us to obviate site-specific river dispersion modelling calculations between the hospital and the WWTP in favour of a more generic type of screening methodology,

especially in the present case in which (as will be seen below) the radiological impact, even with this assumption, is not significant.

It is assumed that the WWTP has a certain flow of water going through it, ϕ_{WWTP}, which is less than the total flow of the river - the water going through the WWTP is in fact 1.1% of the total river flow, if we assume a typical throughput of 1000 m^3 per day in a river of mean flow of 1.0247 m^3 s^{-1} as is typical of the Molse Nete river. The entire radioactivity released by the hospital therefore is assumed to come into the WWTP and what exits back to the river determines the river radioactivity concentration, which should match what was measured by FANC near the outlet.

The apportioning of the incoming (average) radionuclide concentration [Bq m^{-3}] between the various compartments is as follows. For a blocked sewer, it is assumed that 1 month-worth of discharges are trapped in a pipe blockage, as previously espoused elsewhere (McDonnell, 2004). We take the following equation:

$$C_{blocked\ sewer}[Bq\ m^{-3}] = \frac{A_M[Bq]}{V_{blockage}[m^3]} \times \frac{1}{\lambda T} \times f_{blocked\ drain}$$

Where λ is the decay constant, T = 30 days (the factor $\frac{1}{\lambda T}$ is the result of averaging $e^{-\lambda t}$ between 0 and T to correct for ongoing decay during the 30 days, assuming that λT >>1: $A_{avg} = \frac{1}{T}\int_0^E A_0 e^{-\lambda t}dt = \frac{A_0}{\lambda T}\left(1 - e^{-\lambda t}\right) \approx \frac{A_0}{\lambda T}$. Moreover, $f_{blocked\ drain}$ is the % of activity ending in the blockage divided by 100. In other words, the model assumes that a single month's discharge is contained in a small volume (2 m^3) of sewage at a point where the drains have been blocked, with workers operating in the vicinity, whilst undergoing decay. The volume estimation is a best judgement assumption (Titley et al., 2000).

For the WWTP water streams, we simply consider:

$$C_{WWTP}[Bq\ m^{-3}] = \frac{12A_M/s_y[Bq\ y^{-1}]}{\emptyset_{WWTP}[m^3y^{-1}]} \times f_{reaching\ WWTP}$$

Where $12A_M/s_y$ is simply the average annual discharge rate in Bq s^{-1} (A_M is the monthly discharge and s_y is the number of seconds in a year).Therefore, for the WWTP sludge, we have:

$$C_{WWTP\ sludge}[Bq\ m^{-3}] = \frac{12A_M/s_y[Bq\ y^{-1}]}{\emptyset_{WWTP}[m^3y^{-1}] \times r_s[-]} \times f_{in\ sludge\ at\ WWTP}$$

Where r_s is the annual rate of sludge production to incoming sewage = sludge yearly production rate [m^3 y^{-1}] per unit of total incoming sewage flow rate [m^3 y^{-1}].

For the aquatic pathways, the average activity concentration in river water after release is:

$$C_{RW}[Bq\ m^{-3}] = \frac{12A_M/s_y[Bq\ y^{-1}]}{\emptyset_{river}[m^3y^{-1}]} \times (1 - \varepsilon_{WWTP})$$

Where ε_{WWTP} is the removal efficiency of the WWTP. There are three cases of river flow rate that in our calculations are assumed to have the same water concentrations: Water for fish and the calculation of the various external exposure pathways such as irrigation and public drinking water supply. Different values for these pathways could be introduced if the need arises. It is assumed here that the measured activity concentrations supplied to us by the Regulator, being so close to the plant, reflect the concentration of the undiluted effluent (a conservative assumption).

Note that an improvement to this methodology would be to introduce decay terms to account for the time delay in the sewage plant. Decay during transit is ignored in this study because the dose rates are so low that it does not seem necessary to undergo the complication to calculate to that level of detail. Indicative delays that could be used are 0.5 day for milk consumption, 182 days for root vegetables and 7 days for all other foodstuffs (Titley et al., 2000).

5.2.2 Calculation of concentrations for the irrigation and sludge fertiliser pathways

For the irrigation pathway, the starting point is the radionuclide concentration in water C_{RW} [Bq m^{-3}], the Irrigation water flux $\emptyset_W$ [m^3 m^{-2} s^{-1}], the active depth of contamination (average root soil depth for food vegetables) d [m] and the surface area of the soil = S [m^{-2}]. The amount of water infiltrating in the soil per unit time is given by the infiltration equation, which takes into account the (higher) pore water velocity ($v_p = v/\vartheta$ where θ is the volumetric water content of the soil) compared with the irrigation water infall rate: $\frac{dV}{dt} = \frac{\emptyset_W S}{\theta}$ [m^3 s^{-1}]. The rate of change of radionuclide in soil, C$_{soil}$ [Bq] due to infiltration is $\frac{dC}{dt}\big)_{inf} = C_{RW}\frac{dV}{dt} = \frac{C_{RW}\emptyset_W S}{\theta}R$ [Bq s^{-1}]. Here, $R = \left[1 + \frac{\rho K_d}{\theta}\right]^{-1} = \left[1 + \frac{\rho_p(1-\varepsilon)K_d}{\theta}\right]^{-1}$ is the retardation factor, introduced to consider that the radionuclide may be infiltrating at a lower velocity than the water, due to sorption processes as the dissolved radionuclide migrates downwards across the soil column. The additional parameters in this equation are the soil/water distribution coefficient K_d [m^3 kg^{-1}] and the volumetric water content θ [-]. The porosity can be expressed as $\varepsilon = 1 - \frac{\rho}{\rho_0}$ where ρ is the bulk density of the soil and ρ$_p$ is the (higher) particle density (both in kg m^{-3}).

Since the radionuclide is fast decaying, at equilibrium, this has to equal the loss due to decay, which according to the definition of radioactive decay is proportional to the decay constant: $\frac{dC}{dt}\big)_{decay} = \lambda C_{soil}Sd$ [Bq s^{-1}]. Here, C_{PW} is the activity concentration in soil pore water [Bq m^{-3}], S is the surface area and d is the active depth of the contamination. Therefore, $\frac{dC}{dt}\big)_{inf} = \frac{dC}{dt}\big)_{decay} \Rightarrow \frac{C_{RW}\emptyset_W S}{\theta}R = \lambda C_{PW}Sd$. Hence, we arrive at $C_{PW} = \frac{1}{\theta+\rho K_d}\left(\frac{C_{RW}\emptyset_W}{\lambda d}\right)$.

The concentration in soil under conditions of equilibrium can be obtained as $C_{soil} = C_{PW}K_d$, and the concentration in the vegetables is obtained using by further multiplication by the concentration ratio CF [m^3 kg^{-1}]: $C_{veg} = C_{soil}CF = C_{PW}K_d CF$. Thus, the food concentration is $C_{veg} = \frac{1}{\theta+\rho K_d}\left(\frac{C_{RW}\emptyset_W}{\lambda d}\right)K_d CF$, so we finally obtain a food activity per unit deposited activity ratio R [Bq/kg per 1 Bq/m^2 per second] of $R = \frac{C_{veg}}{C_{RW}\emptyset_W} = \frac{1}{\theta+\rho K_d}\left(\frac{K_d CF}{\lambda d}\right)$.

In this project, we used the following element-independent reference biosphere parameters as input for the equations, consistent with the near-surface disposal project for category A waste at Dessel, Belgium (Sweeck, 2018): Volumetric water content θ = 0.32 (general case); average root soil depth d = 0.3 m; soil bulk density ρ = 1350 kg m^{-3}, soil particle density ρ = 2650 kg m^{-3} and, therefore, a porosity 1-ρ/ρ$_p$ of 0.491.

The soil activity per unit deposition arising from a concentration in sludge C$_{sl}$ [Bq kg^{-1}], which is being applied to farmland at a rate $\emptyset_{sl}$ [kg m^{-2} s], is calculated as follows. The rate of change of radionuclide activity in soil, A$_{soil}$ [Bq] due to sludge deposition is: $\frac{dA_{soil}}{dt} = C_{sl}\emptyset_{sl}S$ [Bq s^{-1}], where S is the surface area of the soil. Here again we assume that influx is cancelled by decay, and therefore $C_{sl}\emptyset_{sl}S = \lambda C_{soil}\rho_{soil}Sd \Rightarrow C_{soil} = \frac{C_{sl}\emptyset_{sl}}{\lambda d\rho_{soil}}$ (here, the term $C_{soil}\rho_{soil}Sd$ is the activity concentration in soil multiplied by the mass of the soil, to convert it to units of absolute activity). Frome here we can define a convenient soil concentration per unit deposition ratio $CPUD_{soil} = \frac{C_{soil}}{C_{sl}\emptyset_{sl}} = \frac{1}{\lambda d\rho_{soil}}$ [Bq kg^{-1} per unit Bq m^{-2} s^{-1}], which can be used for the calculation of irrigation dose rates, as shown in Section 5.3.

5.2.3 Calculation of dose rates to maintenance and sewage workers

In order to obtain dose rates, one multiplies the radionuclide concentration by the dose coefficient for internal exposure via inhalation or ingestion (internal dose rate) or by the dose coefficient exposure to ground surface or immersion (external dose rate), and by additional factors as described in turn below.

For accidental ingestion, one must consider the radionuclide concentration in a blocked sewer for maintenance workers, or the average of concentration into sewage works + in sludge at the WWTP for regular workers [Bq m⁻³]. For the latter case, is assumed that workers spend 50% of their yearly working time in each operation. The pertinent activity concentration in sludge [Bq m⁻³] is then divided by the density (approximated by the density of water) to convert the concentration to units of Bq kg⁻¹. Then, the result is multiplied by the ingestion rate [kg h⁻¹], the fractional occupancy f_{occ}^{worker} for the relevant type of worker [h y⁻¹] and the internal dose coefficient via ingestion DC$_{ing}$ [Sv Bq⁻¹], leading to the equation:

$$H_{ing} = \frac{C[\text{Bq m}^{-3}]}{\rho[\text{kg m}^{-3}]} \times DC_{ing}[\text{Sv Bq}^{-1}] \times I_R[\text{kg h}^{-1}] \times f_{occ}[\text{h y}^{-1}]$$

For inhalation, the approach used here takes the activity concentration [Bq m⁻³] (concentration in untreated sewage/sludge for regular workers – assumed to spent 50% of time in each operation) and divides it by the water density to convert the concentration to units of Bq kg⁻¹ of sludge. This is then multiplied by the airborne particulate matter concentration γ_P [kg m⁻³] assuming conservatively that these particles become inhaled, giving the Bq in the particles per unit volume of air. This is then multiplied by the inhalation rate B$_R$ [m³ h⁻¹], the fractional occupancy for the relevant type of worker [h y⁻¹] and the internal dose coefficient via inhalation DC$_{inh}$ [Sv Bq⁻¹], leading to the following equation:

$$H_{inh} = \frac{C[\text{Bq m}^{-3}]}{\rho[\text{kg m}^{-3}]} \times \gamma_p[\text{kg m}^{-3}] \times DC_{inh}[\text{Sv Bq}^{-1}] \times B_R[\text{m}^3 \text{ h}^{-1}] \times f_{occ}^{worker}[\text{h y}^{-1}]$$

For external gamma exposure, the dose rate is proportional to the surface density of contamination [Bq m⁻²]. The dose rate derives from the activity concentration [Bq m⁻³] (in a blocked sewer for maintenance workers, and mean of WWTP water and sludge for regular workers – which assumes 50% of time spent in each operation) multiplied by the contamination depth [m], the occupancy fraction for the worker's task [h y⁻¹], the external dose coefficient [Sv m² s⁻¹ Bq⁻¹] and time units conversions:

$$H_{ext} = DC_{ext}[\text{Sv m}^2\text{s}^{-1}\text{Bq}^{-1}] \times C[\text{Bq m}^{-3}] \times d[m] \times f_{occ}^{worker}[\text{h y}^{-1}] \times y_h[\text{y h}^{-1}] \times s_y[\text{s y}^{-1}]$$

Where y_h and s_y are the unit conversion factors for hours in a year and seconds in a year.

5.3 Calculation of dose rates to the public for the freshwater pathways

In this case, it is necessary to calculate first the river input rate data from Deliverable 3.4 (Fiengo Pérez et al., 2022): $I_{river}[\text{MBq y}^{-1}] = C_{river}^{avg}[Bq\ m^{-3}] \times \varphi_{river}[m^3\ s^{-1}] \times s_y[\text{s y}^{-1}] \times 10^{-6}$. The external gamma dose rate for riverbank occupancy assumes that the riverbank concentration is the riverbed concentration, obtained by multiplication of the average water concentration by the K$_d$. The fraction $\frac{1}{1+S_{susp}K_d}$ is a factor used to take water filtration into account. Hence:

$$H_{ext}[\text{Sv y}^{-1}] = \frac{1}{1+S_{susp}K_d} C_{river}^{avg}[Bq\ m^{-3}] \times K_d[m^3\ kg^{-1}] \times f_{occ}^{riverbank}[\text{h y}^{-1}] \times$$
$$DC_{groundsurf}^{ext}[Sv\ Bq^{-1}\ s^{-1}\ m^2] \times d[m]x\ \rho_{soil}^{bulk}[kg\ m^{-3}] \times y_h[\text{y h}^{-1}] \times s_y[\text{s y}^{-1}].$$

The ingestion dose rate arising from fish consumption is as follows:

$$H_{ing}^{fish}[\text{Sv y}^{-1}] = \frac{CR_{fish}[kg\ kg^{-1}]}{\rho_w[\text{kg m}^{-3}]} \times \frac{C_{river}^{avg}[Bq\ m^{-3}]}{1+S_{susp}K_d} \times I_r^{fish}[kg\ y^{-1}] \times DC_{ing}[\text{Sv Bq}^{-1}]$$

In addition, for the ingestion of drinking water and unfiltered river water:

$$H_{ing}^{drwater}[\text{Sv y}^{-1}] = \frac{C_{river}^{avg}[Bq\ m^{-3}]}{1+S_{susp}K_d} \times I_r^{drwater}[m^3\ y^{-1}] \times DC_{ing}[\text{Sv Bq}^{-1}]$$

$$H_{ing}^{unfwater}[\text{Sv y}^{-1}] = C_{river}^{avg}[Bq\ m^{-3}] \times I_r^{drwater}[m^3\ y^{-1}] \times DC_{ing}[\text{Sv Bq}^{-1}]$$

5.4   Calculation of dose rates to the public arising from the agricultural use of sludge

As seen above, $C_{soil}[Bq\ kg^{-1}] = CPUD_{soil}[m^2\ s\ kg^{-1}] \times C_{sl}[Bq\ kg^{-1}] \times \emptyset_{sl}[kg\ m^{-2}s^{-1}]$. This can be converted to external dose rate (internal exposure is negligible) by means of the following equation:

$$H_{ext} = DC_{ext}[\text{Sv m}^2\text{s}^{-1}\text{Bq}^{-1}] \times C_{soil}[\text{Bq kg}^{-1}] \times \rho[\text{kg m}^{-3}] \times d[m] \times f_{occ}^{farmland}[\text{h y}^{-1}]$$
$$\times\ y_h[\text{y h}^{-1}] \times s_y[\text{s y}^{-1}]$$

6   Assessment for wildlife

6.1   Routine scenario

6.1.1   Activity concentrations in water, sediment, and the wildlife

Activity concentrations for the 6 radionuclides considered in the river at the plant outlet, as modelled in D3.4 (Fiengo Pérez et al., 2022), and the resulting activity concentration (calculated dynamically using the D-DAT model) in the upper layer of the riverbed sediment (assumed to be 5-cm), are given in Fig. 14. The levels in river water assume extraordinary circumstances such as maintenance or expansion (especially in the WWTP) whereupon effluents could be directly released into watercourse under conditions of low flow. Such circumstances can occur and must be included in the assessment.

The activity concentrations in water exhibit daily fluctuations that are related to the activities of the hospitals. The principal radionuclides in terms of activity concentration in water (by two orders of magnitude) are ^{201}Tl, followed by [123/131]I and ^{99m}Tc, ^{18}F and the remainder. For sediment, the order is ^{201}Tl, [153]Sm, then ^{131}I and ^{99}Tc, ^{18}F and the remaining radionuclides. The time-integrating action of the sediment smoothens somewhat the oscillating water radionuclide levels, especially for ^{201}Tl and [153]Sm.
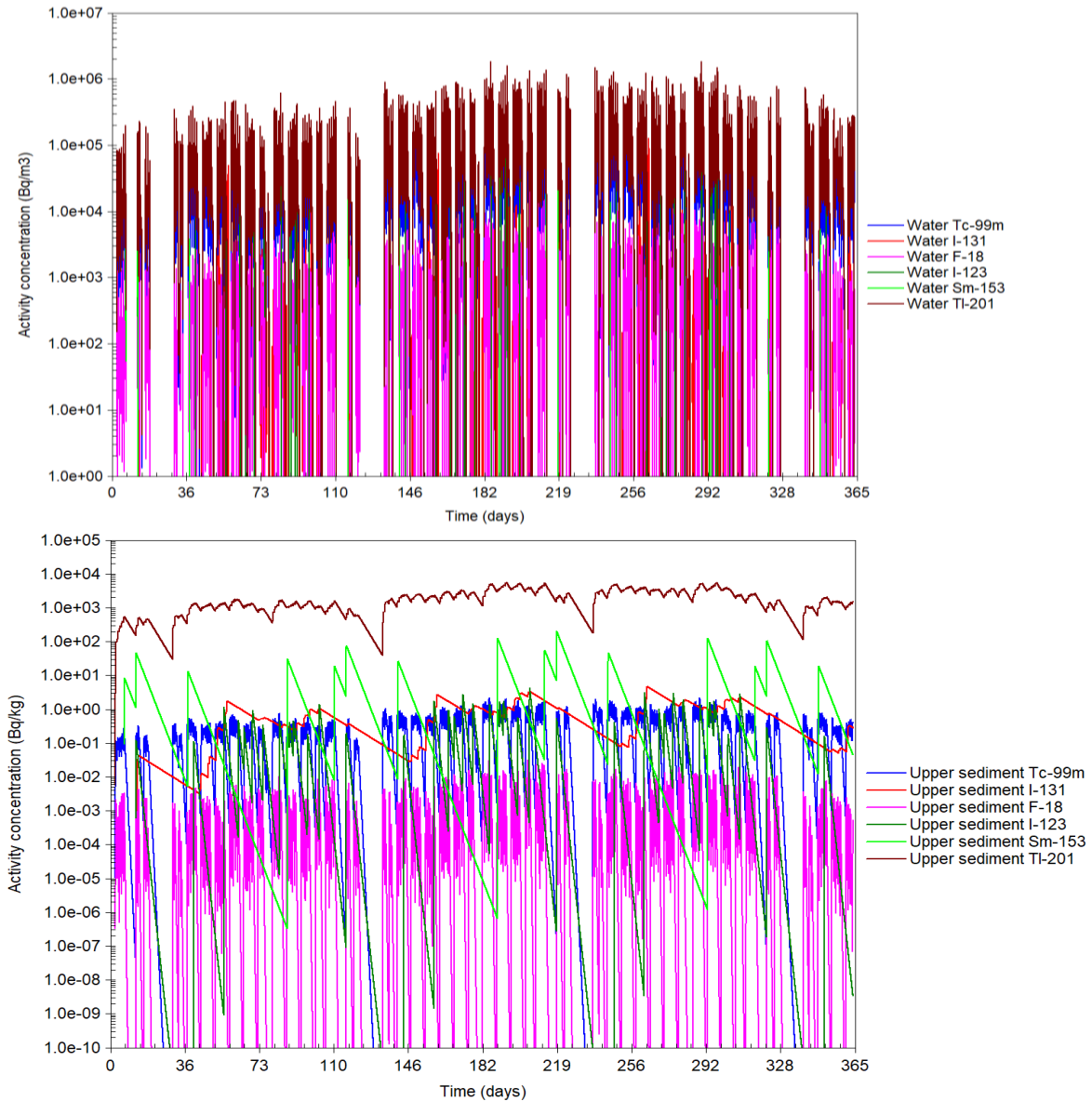
Figure 14: Activity concentrations in Molse Nete river water (above) and sediment (below) at the outlet of the local WWTP in 2018

For the calculation of activity in sediment, we used a reworking rate for the turnover of the upper bed sediment of 1.37×10^{-5} m d^{-1}, typical of shallow environments (Simmonds et al., 2004).

Figure 15 gives the dynamically modelled activity concentration of ^{18}F, ^{99m}Tc, ^{123}I, ^{131}I, ^{153}Sm, and ^{201}Tl in pelagic & benthic fish, crustaceans, mollusc, macro-algae, phytoplankton, and zooplankton. From this figure, it can be seen that ^{18}F, ^{99}Tc, ^{153}Sm and ^{201}Tl concentrate principally in plankton, whereas for ^{123}I and ^{131}I, the radionuclide concentrates principally in fish. The activity concentrations display maxima in the order of magnitude 10^6 (^{201}Tl), 10^4 (^{18}F, ^{99}Tc and ^{153}Sm) and 10^3 ($^{123/131}$I) Bq kg^{-1}.

The transfer parameters used to derive the above activity concentrations are detailed in Section 3. We used data from the ERICA Tool, either primary data or applying the Tool's deductive method based on analogues. For some radionuclides (in our assessment, this concerns I and Tc) there is an additional source containing element dependent environmental input parameters for the Category A waste disposal in Belgium (Sweeck, 2022), including some transfer parameters that cannot be found in IAEA

TRS472 (IAEA, 2010). The reported K_d values for these radionuclides are 10^{-1} and 1.0×10^{-2} m^3 kg^{-1}, respectively (or 3.6 m^3 kg^{-1} if Mo and Tc are considered as analogues, as recommended here). Whilst drawing attention to this source, we retain the results obtained with the ERICA method because (a) the values used are either similar or more conservative, (b) there is consistency with the calculation approach for the other radionuclides for which there are no data in the Belgian source, and (c) an assessment for a European scenario would tend to use the ERICA values. A similar situation occurs for the concentration factors. The Belgian CF for fish is 10^{-1} m^3 kg^{-1} for I and 1.5×10^{-2} for Tc, compared with the values in our database of 3.1×10^{-1} and 9.9×10^{-2} m^3 kg^{-1}, respectively, which again implies a higher degree of conservatism for the parameters in our database, as desired.

6.1.2   Dose rates to the wildlife

The dynamically modelled dose rates of ^{18}F, ^{99m}Tc, ^{123}I, ^{131}I, ^{153}Sm, and ^{201}Tl to pelagic & benthic fish, crustaceans, mollusc, macro-algae, phytoplankton, and zooplankton (unweighted by radiation quality) are given in Fig. 16. This figure gives the total dose rate, summing of internal and external exposures (according to our simulations, internal exposure dominates over external by 2 − 3 orders of magnitude). The peaks in Figure 16 have absolute maximum values of the order of magnitude 10^{-1} (^{99}Tc, $^{123/131}$I, ^{153}Sm), 10^{0} (^{18}F) and 10^{1} (^{201}Tl) µGy h^{-1}.

In a dynamic situation like the one considered, peak maximum dose rates are not a meaningful quantity to measure the risk, because such dose rates are applied over a short time and lower dose rates prevail for most of the time. Rather, it is the integration of the dose rate received over a set time divided by the time, i.e. the average dose, that should be used to compare with benchmark values of dose. The D-DAT model performs such a calculation for a time of 1 year, as shown in Fig. 17. This figure is to be interpreted as follows. For a given time T, the output is the average dose rate between t = zero and t = T, divided by T. In particular, we take the last point in the graph (T = 365 days) to give an average dose rate for the period.

The following conclusions are evident from Figure 17. Firstly, external exposures (in the order macroalgae > mollusc > benthic fish > phytoplankton and zooplankton > pelagic fish) are several orders of magnitude below internal exposures, which are in the order mollusc > phytoplankton > crustacean and benthic fish > zooplankton and pelagic fish > macroalgae. Secondly, the highest annually averaged dose rate (internal dose rate for mollusc, arising mainly from ^{201}Tl), at 3.7 µGy h^{-1}, is below the 10 µGy h^{-1} incremental screening dose rate for risk characterisation from the ERICA methodology (Brown et al., 2016; Brown et al., 2008), with a risk quotient of 0.37.

The object of protection within the ERICA Integrated Approach is that generic ecosystems are protected from structure and function effects under chronic exposures. The ERICA methodology proposes the aforesaid 10 µGy h^{-1} screening dose rate based on examination of data on effects of ionising radiation in wildlife (Copplestone et al., 2008; FREDERICA, 2006). This is not a limit: exceeding it means simply that the site under analysis cannot be screened-out from further detailed assessment.
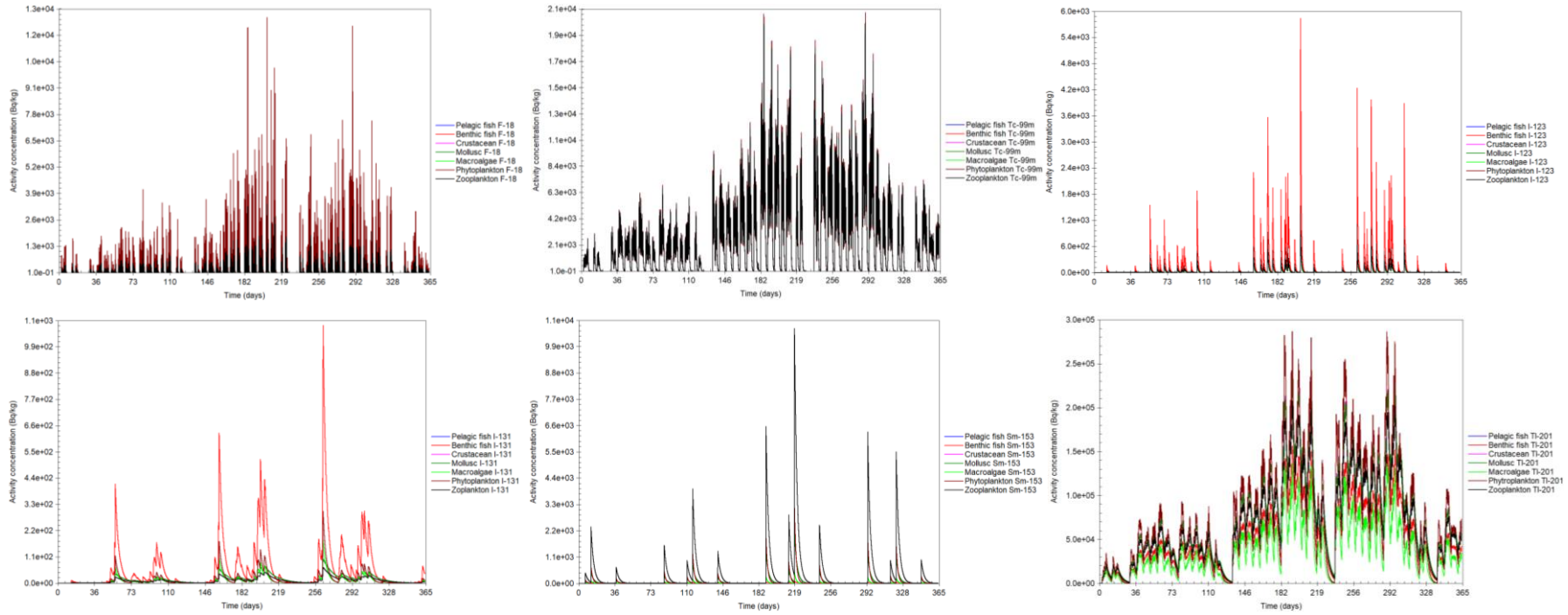
Figure 15: Dynamically modelled activity concentration of radionuclides in aquatic wildlife from the Molse Nete River
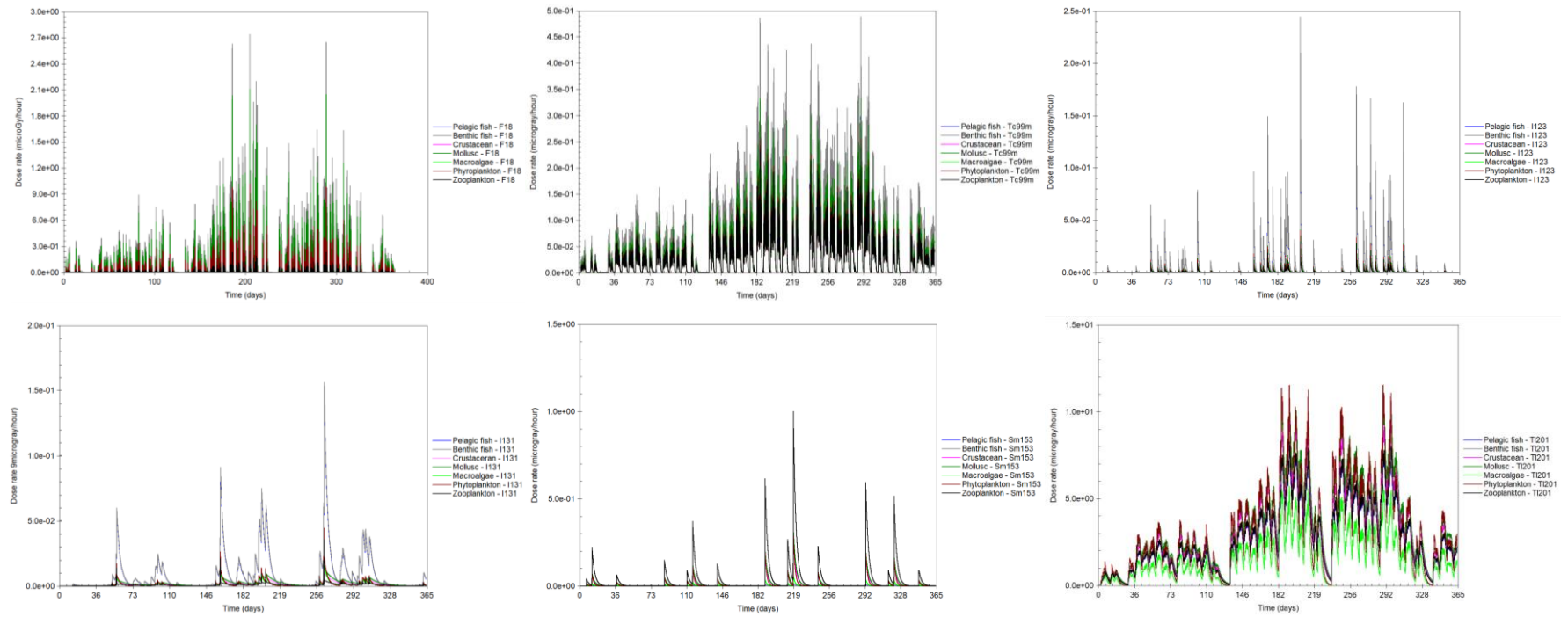
Figure 16: Dynamically modelled dose rates of radionuclides in aquatic wildlife from the Molse Nete River
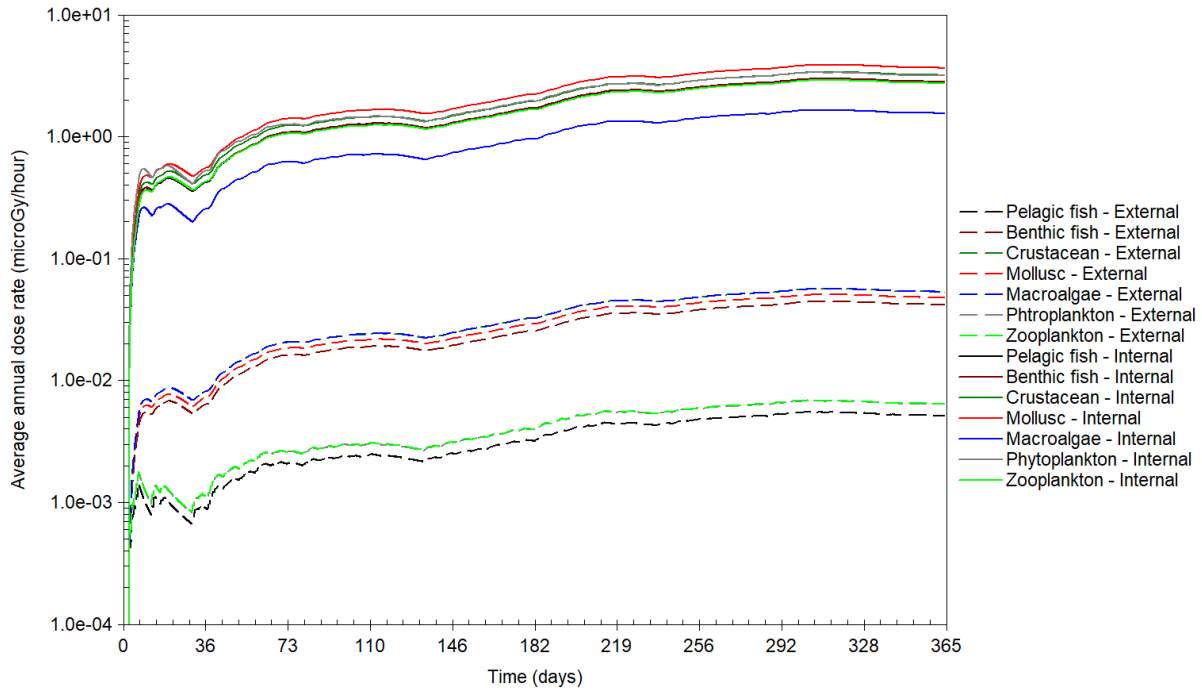
Figure 17: Integration of internal and external dose rates (sum of all radionuclides) over a one-year period, divided by the time period considered

The information, given in Table 1, shows significant decay in transit after a few kilometres downstream from the plant, particularly for ^{18}F, ^{99m}Tc and ^{123}I. For the other radionuclides, decay in transit is minor.

Table 1: Attenuation factors at varying distances from the WWTP for the Molse Nete 2018 scenario

Distance (m)	Time (s)	^{18}F	^{99m}Tc	^{123}I	^{131}I	^{153}Sm	^{201}Tl
0	0.00E+00	1	1	1	1	1	1
10	1.79E+01	99.81%	99.94%	99.97%	100.00%	99.99%	100.00%
100	1.79E+02	98.14%	99.43%	99.74%	99.98%	99.93%	99.95%
1000	1.79E+03	82.87%	94.45%	97.43%	99.82%	99.27%	99.53%
10000	1.79E+04	15.27%	56.49%	77.07%	98.23%	92.90%	95.40%
$T_{1/2}$ (s)		6.59E+03	2.17E+04	4.75E+04	6.95E+05	1.68E+05	2.63E+05

In our case, it is possible to state that the aquatic biota at the outlet of the WWTP are not at risk, considering that the dose rates are in any case well below the lower level of the ICRP derived consideration reference level (DCRL) bands for biota (ICRP, 2008).

In reality, the calculated dose rates to biota are conservative, due to the following assumptions (a) that the WWTP is temporarily out of operation and the sewage flow is diverted to river, and (b) that we have calculated doses for the most exposed organisms in the vicinity of the plant (whereas biota populations span the river as a whole, and radionuclides decay during transport downstream). Using our hydrological modelling results, we established that the water velocity for the Molse Nete in 2018 varied spatially (between 0 and 1% variability in these four locations) and, most significantly, temporally (from 0.23 to 0.56 m s^{-1}). The case of maximum velocity implies that the radionuclides are transported further away with relatively less decay in transit. For the purposes of illustration, we

calculated attenuation coefficients $f = e^{-\frac{\ln(2) \times t}{T_{1/2}}}$ due to radioactive decay at various distances from the discharge point using a velocity is 0.56 m s^{-1}.

6.2 Accidental ^{131}I release scenario

6.2.1 Activity concentrations in water, sediment and the wildlife

Fig. 18 gives the activity concentration in water and sediment per MBq ^{131}I release directly into the sewer system (iodine pill release scenario), reaching the river at the outlet of the WWTP during plant shutdown when the river carries the lowest flow. This scenario can be scaled-up if desired, as the doses are proportional to release. The resulting time-dependent and time-averaged dose rates are given in Fig. 19. In this Figure, we have placed the peak at T = zero in order to be able to follow-up the decaying dose profile over a 1-year period after release. The 1-year averaging cut-off time is arbitrary of course, but dose rates for different integration periods can be extrapolated if desired from the given figures.
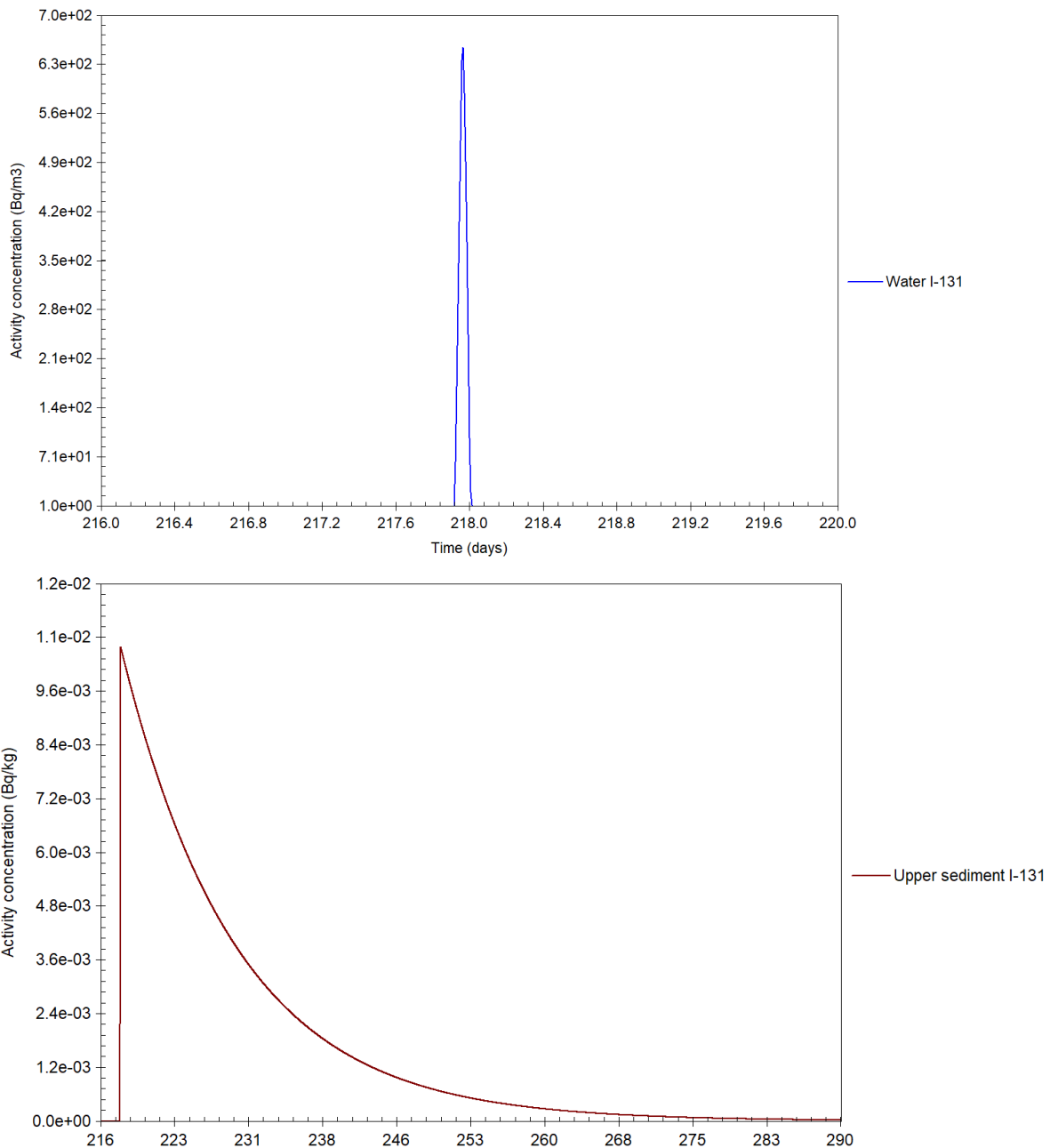
Figure 18: Modelled activity concentrations of ^{131}I in water (above) and sediment (below) for the accidental iodate pill release scenario
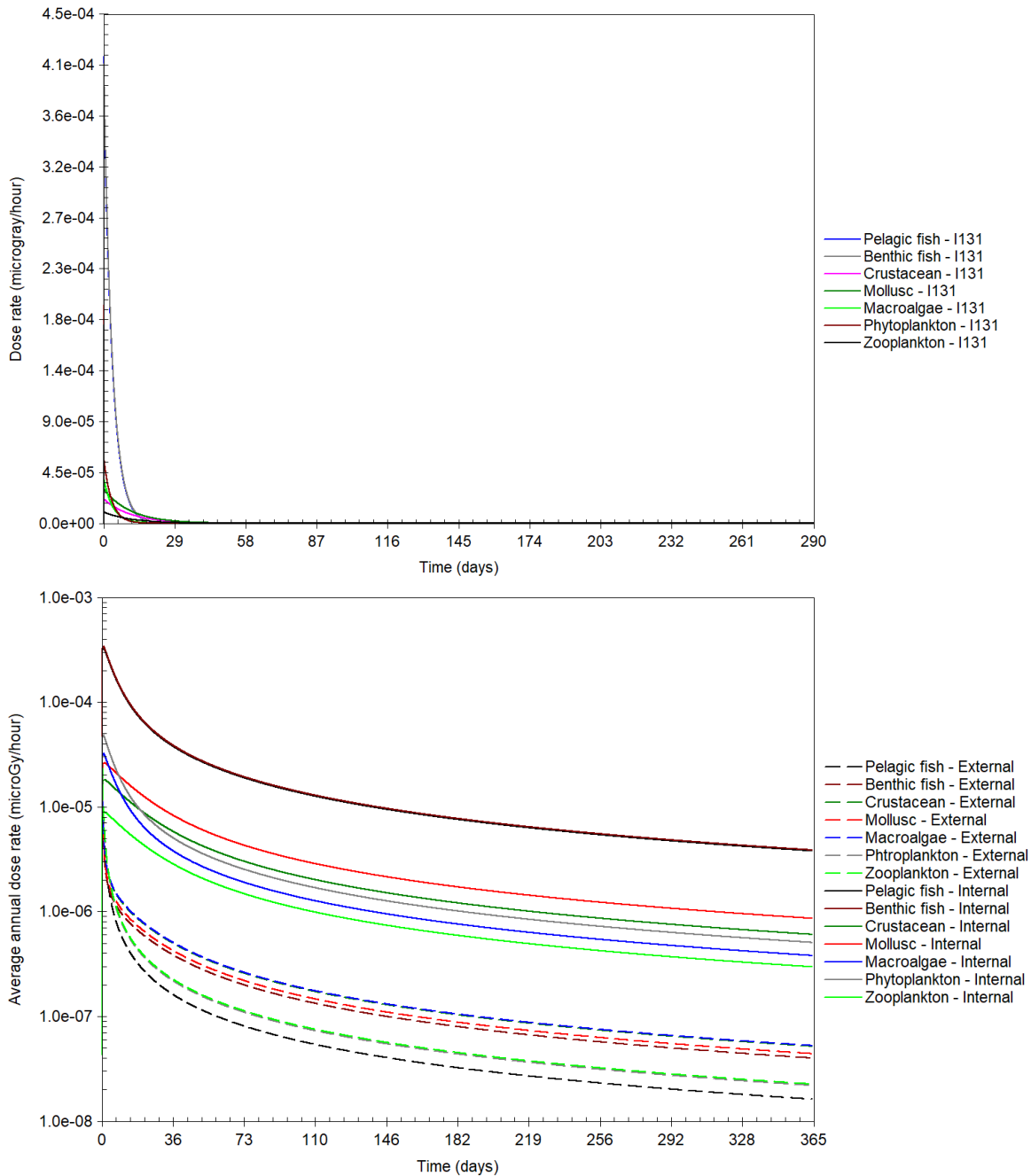
Figure 19: Modelled ^{131}I in dose rate in biota (above) and integration of internal and external dose rates (sum of all radionuclides) over a one year period following release, divided by the time period considered for the accidental iodate pill release scenario (below)

The conclusion that the exposures to non-human biota have no radiological significance whatsoever can be determined by consultation of these figures. The single peak of water concentration, with a maximum of 654 Bq m^{-3} at the WWTP outlet at T = 218 days and associated peak in sediment of a maximum of 0.011 Bq kg^{-1}, rapidly decay through the effects of delay and dilution. The maximal activity concentration in biota is 218 Bq kg^{-1} for pelagic and benthic fish, with progressively lower concentrations of phytoplankton, macroalgae, crustacean and zooplankton (in that order).

6.2.2 Dose rates to the wildlife

The peak doses to the biota are of the order of 4.1 × 10^{-4} µGy h^{-1} for pelagic and benthic fish followed by phytoplankton > macroalgae > crustacean and mollusc > zooplankton (Fig. 19). The one-year time-averaged dose rates are very low. For internal exposure, they are 4 × 10^{-6} µGy h^{-1} for pelagic and benthic

fish, decreasing to 9×10^{-7} µGy h^{-1} for mollusc, 6×10^{-7} µGy h^{-1} for crustacean, 5×10^{-7} µGy h^{-1} for phytoplankton, 4×10^{-7} µGy h^{-1} for macroalgae and 3×10^{-7} µGy h^{-1} for zooplankton. External dose rates are one order of magnitude lower with the most exposed group being macroalgae, with a very low dose rate of 5×10^{-8} µGy h^{-1}, and the least exposed group being pelagic fish at $< 2 \times 10^{-8}$ µGy h^{-1}. According to the methodology used here, such dose rates have no environmental significance. Hence, this type of accidental release scenario poses no significant risk to the environment.

7 Assessment for people

7.1 Doses to consumers and members of the public using the D-DAT dynamic model

The D-DAT model was used to calculate the dose rates to people of three age groups (adult, 10-year-old and infant) arising from ingestion of water and of the biota, once consumption rates are set. The results are given in Fig. 20. D-DAT was also used to calculate the external dose rates from sediment (walking along the riverbank) and swimming exposure, as shown in Fig. 21.

The mean internal dose rates arising from ingestion of biota from the WWTP at the outlet (mainly fish) over a 1-year period range between 2×10^{-6} Sv y^{-1} for child to 8×10^{-6} Sv y^{-1} for infant, the differences being caused by the different dose factors and Belgian consumption rates for the different age groups (reflecting the age-dependent radiation sensitivity). The mean internal dose rates from water ingestion are lower, ranging from 5×10^{-7} Sv y^{-1} for adult to 1×10^{-6} Sv y^{-1} for the infant.

The above dose rates are much lower than the worldwide average annual radiation dose rate from exposure due to naturally occurring radiation sources, including radon, of 2.4 mSv (UNSCEAR, 2000) and very close to 10 µSv y^{-1} which is considered a trivial dose in terms of risk (IAEA, 2014).

In the scenario considered, the dose rates calculated are maximal, under a pessimistic scenario that the sewerage effluent is not treated by the WWTP and is diverted into the river (Fiengo Pérez et al., 2022). In reality, hospital-discharged radionuclides would be conveyed to the WWTP for standard treatment before they are released into the river, and a significant fraction of the radionuclide activity being lost through purification and decay. Further down the river, radionuclide concentrations diminish rapidly due to dilution and decay, indicating an even lower risk. If we add to this the effect of decay during transport of the food to the consumer, it can be seen that these exposures are of no radiological significance whatsoever.

External exposures have the same implications. Exposure to sediment walking along the riverbank ranges between 1.5×10^{-6} Sv y^{-1} for adult and 2×10^{-6} Sv y^{-1} for the infant, due to age-related differences in dose factors. The dose rates for external exposure due to swimming are much lower, between 5×10^{-8} and 6×10^{-8} Sv y^{-1}. These dose rates are essentially trivial.

Water intake and external dose rates to the public were calculated in Deliverable 3.4 (Fiengo Pérez et al., 2022). Comparison is not immediate because we used dynamically calculated average dose rates for a 1-year period, whereas D3.4 gives a preliminary estimation based on maximal concentrations (average of the 8 highest concentrations in the release scenario considered). For the D3.4 and D3.5 overlapping cases of water ingestion and immersion, however, the dose rates are comparable, with a tendency of our estimates to be somewhat lower (as much as one order of magnitude in some cases). In all cases, the conclusions are identical, in that these dose rates are of no radiological significance.

The ^{131}I accident exposure scenario simulation gives significantly lower exposures compared with the routine scenario, as seen in Figs. 22 and 23. As we did in the assessment for biota, we placed the discharge at t = zero to perform integration over a complete year (the averaging cut-off time is arbitrary but doses for different integration periods can be obtained from the Figures). Modelled average dose rates after 1 year are several orders of magnitude below the trivial dose rate of 10 µSv y^{-1} indicating no radiological significance whatsoever for this situation.
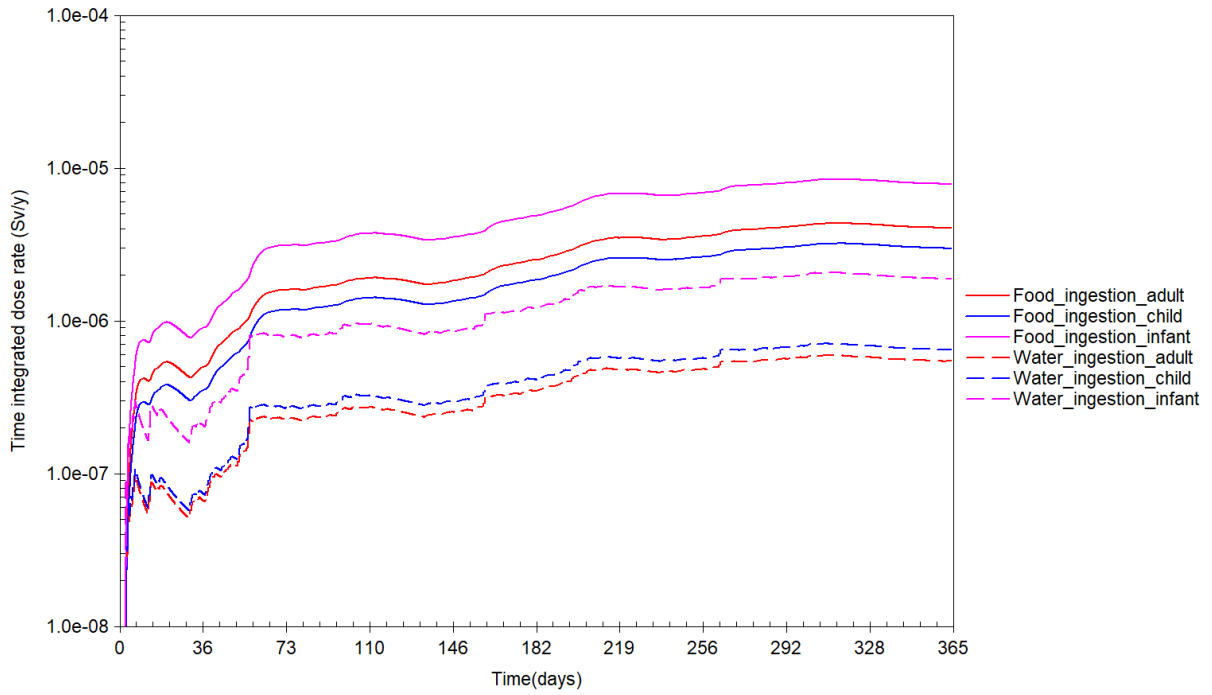
Figure 20: Time integrated ingestion dose rates for a routine discharge scenario, combining all radionuclides and food groups
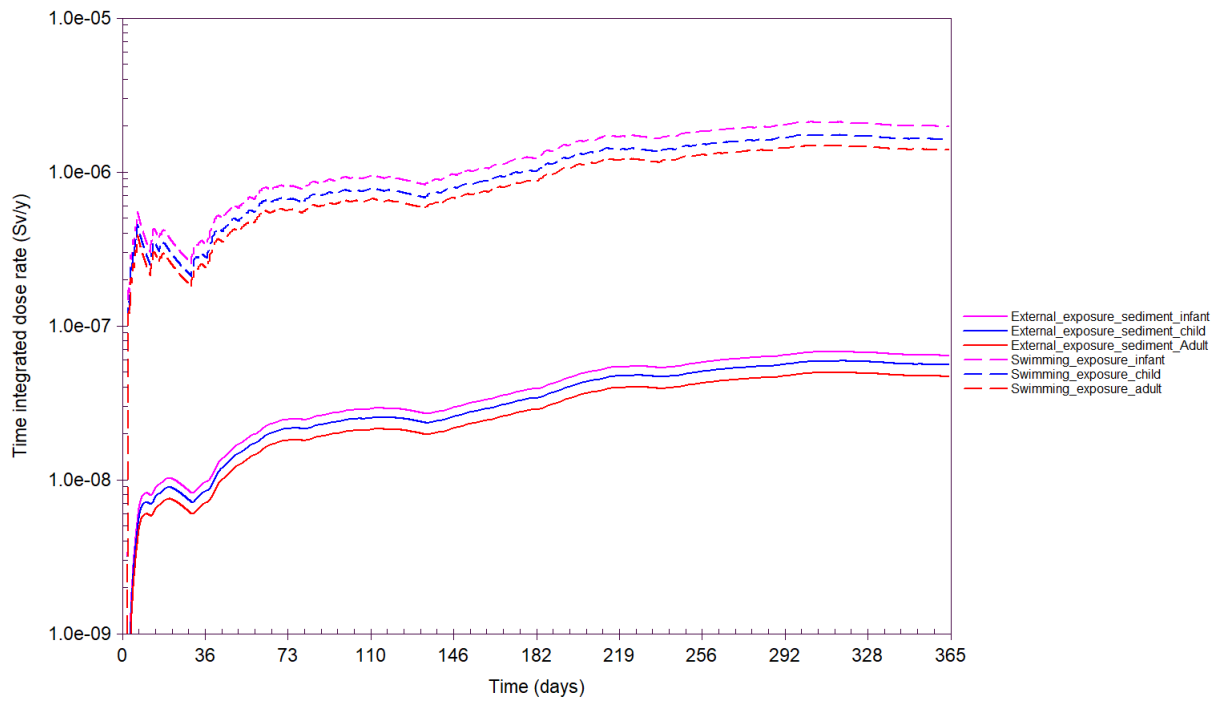
Figure 21: Time-integrated external exposure dose rates for a routine discharge scenario
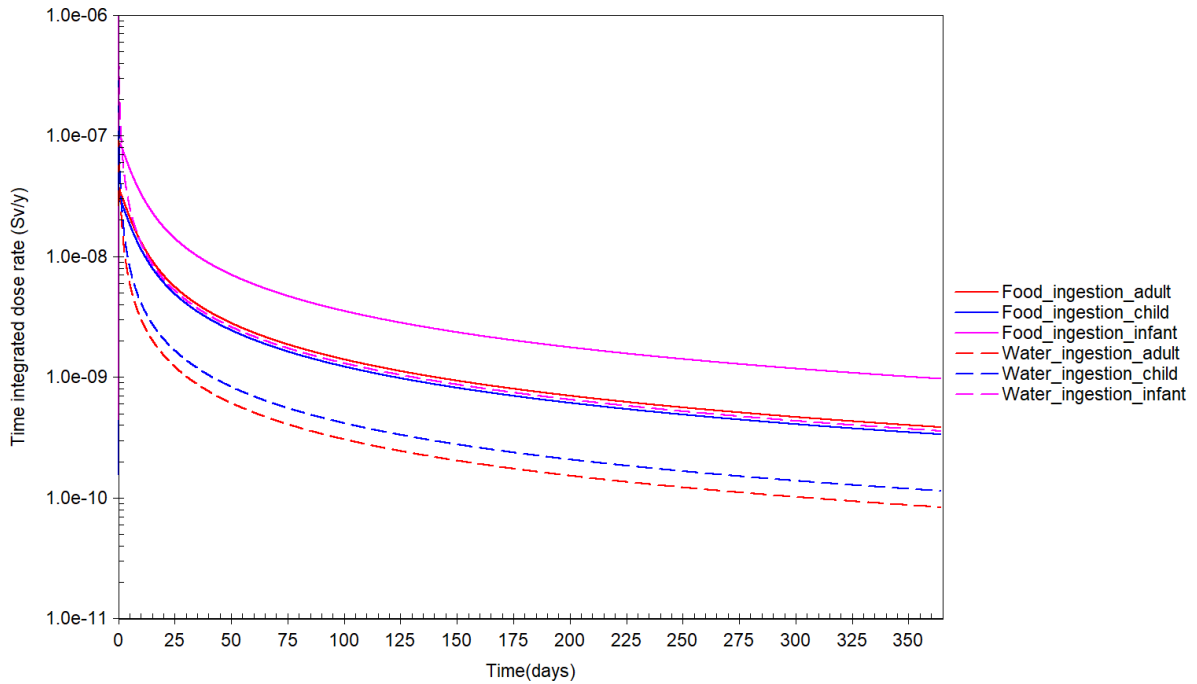
Figure 22: Time integrated ingestion dose rates for an accidental release of ^{131}I, combining all radionuclides and food groups
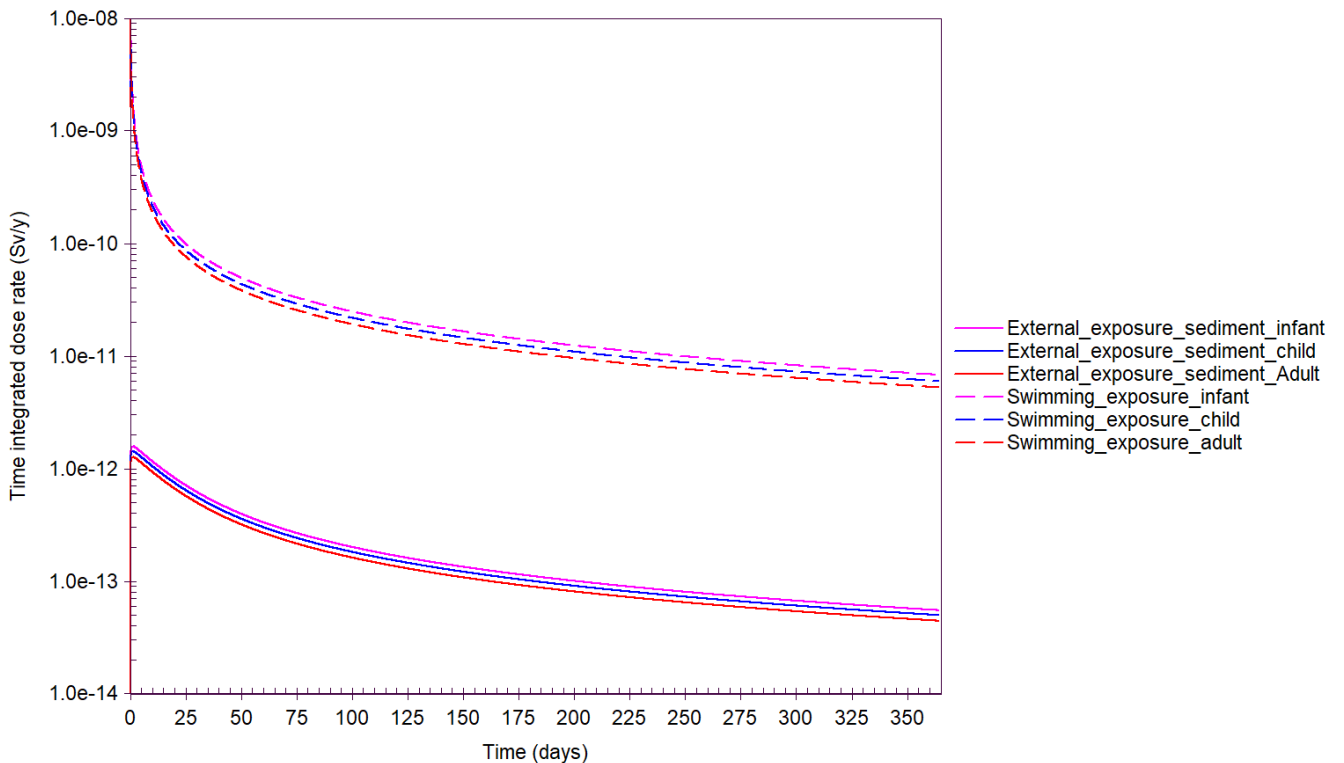
Figure 23: Time-integrated external exposure dose rates for an accidental release of ^{131}I

7.2   Doses to WWTP workers and the public using the WWTP fractionation calculator

7.2.1   Fractionation of radionuclides at the WWTP

Unlike the dynamic assessment for people and biota downstream from the plant, which makes the pessimistic assumption that radionuclides are diverted from the WWTP to the watercourse, a conservative assessment for workers in the plant and the post-WWTP discharge pathway has to

assume that the WWTP is operational. The main source of uncertainty in the dose assessment is the WWTP removal efficiency, that is, fraction of activity concentration entering the plant that is retained and thus separated from the effluent. Hence, the first step was to establish these efficiencies.

The Belgian regulator FANC performed automatic gamma spectrometric measuring stations at both inlet and outlet of several WWTPs in Belgium. This would, in theory, enable calculation of the efficiencies. However, in practice, it is not straightforward to do so because the detection limit was approximately 10^3 Bq m^{-3}, sufficient in principle to detect the main radionuclides associated with hospital discharges (^{99m}Tc, ^{131}I and ^{201}Tl), but not others like ^{18}F, ^{123}I, ^{153}Sm (Fiengo Pérez et al., 2022). For the latter, it would be not possible to reconstruct the true removal efficiency based on detection limits. The problem is compounded by the short half-life of the radionuclides combined with not knowing the transit time of the different effluent fractions – for indicative purposes, a transition time of 15 hours is assumed for liquid effluent and 17 days are assumed for conditioned sewage sludge, which are treated for long enough to make them suitable for application to land (EA, 2022). All these factors can distort the calculation of the removal efficiencies.

In view of the above limitations, we decided that it was preferable to source the (radionuclide-dependent) WWTP fractionation parameters, for which a reference was found in the literature (McDonnell, 2004). The first parameter required is the removal efficiency of the sewage processing, that is, the fraction not exiting the installation (in our study, we assume that there is no loss due to decay during the few hours that the radioactivity is in the WWTP except for ^{18}F, ^{99m}Tc and ^{123}I). The second parameter is the fraction of the initial effluent that ends-up in the produced sludge (incorporating estimated decay in all cases, meaning that the fraction of ^{18}F, ^{99m}Tc and ^{123}I is virtually zero). The data are given in table 2. For ^{18}F and ^{123}I for which the reference gives no data, a 90% efficiency of removal for sewage is assumed by expert judgement, similar to ^{99m}Tc due to considerations of chemistry and fast decay. For ^{153}Sm, the same efficiency as for ^{201}Tl is assumed, based on similar considerations.

Table 2: Fractionation of radionuclides in sewage treatment plants

Radionuclide	Fraction in sewage	Fraction in sludge
^{18}F	0.9	0
^{99m}Tc	0.9	0
^{123}I	0.9	0
^{131}I	0.2	0.05
^{153}Sm	0.8	0.01
^{201}Tl	0.8	0.01

The WWTP assessment was performed using average concentrations because it is too complex now to do otherwise and the data are too limited to perform a dynamic modelling as was done for the non-human biota. Based on the data from Table 2, along with an assumption of 1% of the activity captured in the blocked sewer scenario and the data shown in Figures 8 and 9, we arrived at average activity concentrations in the different WWTP fractions, as shown in Table 3.

Table 3: average activity concentrations in the different WWTP fractions

Radionuclide	Average activity concentration (Bq m^{-3})			
	Blocked Sewer	In liquid at WWTP	In sludge at WWTP	River discharge
^{18}F	4.2E+04	3.8E+04	0.0E+00	4.3E+01
^{99m}Tc	8.3E+06	2.3E+06	0.0E+00	2.6E+03
^{123}I	2.9E+05	3.6E+04	0.0E+00	4.1E+01
^{131}I	2.0E+06	1.7E+04	3.0E+04	1.5E+02
^{153}Sm	1.1E+05	3.7E+03	1.4E+03	8.4E+00
^{201}Tl	3.1E+08	6.9E+06	2.5E+06	1.6E+04

7.2.2 Radiological exposures for the routine scenario

The radiation dose rates to workers at the WWTP (general work) and sewer maintenance workers (repairing a blockage), are given in Table 4. It can be seen that the order of exposure is external gamma > ingestion > inhalation, and that dose rates due to maintenance work are an order of magnitude lower than for general work, mainly due to the lower occupancy rate. It can be seen also that the order of contribution by radionuclide to total exposure is ^{201}Tl > ^{99m}Tc > ^{18}F > ^{131}I > ^{123}I > ^{153}Sm. Given that ^{201}Tl is not a strong gamma emitter, with main gamma emissions of 70.8 keV (46.5%), 68.9 keV (27.4%) and 80.3 keV (20.5%), much of the resulting dose is likely reduced by shielding provided by walls, tanks and containers, leading to very low dose rates for workers. Nevertheless, the highest dose rate (WWTP worker, sum of all radionuclides) is 58 µSv y^{-1}, a small fraction of the dose from naturally occurring radiation sources, including radon, of 2.4 mSv (UNSCEAR, 2000). All maintenance worker doses, and the majority of doses to WWTP workers except the external gamma exposure to ^{99m}Tc and ^{201}Tl , are below the trivial dose level of 10 µSv y^{-1}.

Table 4: Dose rates to workers at the WWTP including general work and sewer maintenance

Radionuclide	Dose rate (Sv y^{-1})			
	Ingestion	Inhalation	External Gamma	Totals
WWTP workers				
^{18}F	1.9E-11	2.5E-12	2.2E-06	2.2E-06
^{99m}Tc	5.0E-10	3.0E-11	1.4E-05	1.4E-05
^{123}I	7.6E-11	2.9E-12	2.8E-07	2.8E-07
^{131}I	1.0E-08	3.8E-10	1.0E-06	1.0E-06
^{153}Sm	3.8E-11	3.5E-12	1.8E-08	1.8E-08
^{201}Tl	8.9E-09	4.6E-10	4.0E-05	4.0E-05
Total	2.0E-08	8.8E-10	5.8E-05	5.8E-05
Maintenance workers				
^{18}F	8.3E-14	1.9E-15	9.9E-09	9.9E-09
^{99m}Tc	7.3E-12	7.8E-14	2.1E-07	2.1E-07
^{123}I	2.4E-12	1.7E-14	9.1E-09	9.1E-09
^{131}I	1.7E-09	1.1E-11	1.7E-07	1.7E-07
^{153}Sm	3.1E-12	5.2E-14	1.5E-09	1.5E-09
^{201}Tl	1.2E-09	1.1E-11	5.2E-06	5.2E-06
Total	2.9E-09	2.2E-11	5.6E-06	5.6E-06

Dose rates for the freshwater pathways are given in Table 5. The dose rates from drinking water, either WWTP treated water or unfiltered river water at the release point, are of no radiological significance whatsoever. The fish ingestion and external gamma radiation doses in Table 5 provide a point of comparison with the doses for the same pathways as dynamically calculated by D-DAT (see Section 7.1). The main difference between the two is that the human dose calculator used here considers removal of a significant part of the radioactivity at the WWTP, whereas the D-DAT model calculation assumes that the radioactivity is diverted directly to the river, whereupon the D-DAT dose rates are more conservative in this respect and should be used as the primary evaluation of the dose because of this factor and because the D-DAT model calculates radionuclide transfer dynamically.

The predicted concentrations for application of water in irrigation and resulting dose rates are shown in Table 6. Dose rates arising from use of WWTP sludge as a ground fertiliser are shown in Table 7. Dose rates from use of sludge as fertiliser predominate over dose rates from irrigation, but in both

cases, the total dose rates (7.1 × 10^{-8} Sv y^{-1} and 2.9 × 10^{-9} Sv y^{-1}, respectively) are insignificant, being below the 10-µSv y^{-1} trivial dose level.

Table 5: Dose rates for the freshwater pathways

Radionuclide	Dose rate (Sv y^{-1})			
	External gamma at the riverbank	Fish ingestion	Drinking WWTP treated water	Drinking unfiltered river water
^{18}F	2.6E-09	1.4E-11	9.2E-10	1.5E-12
^{99m}Tc	4.4E-07	3.6E-11	2.5E-08	4.1E-11
^{123}I	3.8E-07	1.6E-11	3.6E-09	6.2E-12
^{131}I	3.9E-06	6.4E-09	1.4E-06	2.4E-09
^{153}Sm	8.9E-06	2.0E-13	2.2E-10	4.6E-12
^{201}Tl	1.2E-04	3.6E-08	6.1E-07	1.1E-09
Total	1.3E-04	4.2E-08	2.0E-06	3.6E-09

Table 6: Predicted concentrations and resulting dose rates for the irrigation pathway

Radionuclide	Concentrations (Bq kg^{-1})		Dose rates (Sv y^{-1})		Totals
	Green Vegetables	Root Vegetables	Green Vegetables	Root Vegetables	
^{18}F	1.3E-04	6.2E-05	3.0E-13	3.5E-13	6.5E-13
^{99m}Tc	2.2E-01	5.7E-02	2.2E-10	1.5E-10	3.7E-10
^{123}I	1.3E-05	1.3E-05	1.2E-13	3.2E-13	4.5E-13
^{131}I	7.1E-04	7.1E-04	7.0E-10	1.8E-09	2.5E-09
^{153}Sm	1.9E-07	1.9E-07	6.4E-15	1.7E-14	2.3E-14
^{201}Tl	7.4E-03	1.4E-03	3.2E-11	1.5E-11	4.7E-11
Total	2.3E-01	5.9E-02	9.6E-10	2.0E-09	2.9E-09

Table 7: Activity concentration in sludge and dose rates arising from use of WWTP sludge as a ground fertiliser

Radionuclide	Concentration (Bq kg^{-1})	Dose rate (Sv y^{-1})
^{18}F	0.0E+00	0.0E+00
^{99m}Tc	0.0E+00	0.0E+00
^{123}I	0.0E+00	0.0E+00
^{131}I	3.0E+01	1.0E-08
^{153}Sm	1.4E+00	1.8E-11
^{201}Tl	2.5E+03	6.1E-08
Total	2.5E+03	7.1E-08

7.2.3   Radiological exposures for the accidental scenario

For the accidental scenario, this method of calculating dose, based on a time average, is not naturally suited for a assessing a single isolated pulsed discharge. The integration period is by its nature arbitrary. In order to derive the average dose rate over the integration period, there is a need to use the average activity concentration in water for that period. The time integrated dose rate is calculated and divided by the number of days of the integration period. For consistency with what was done in the routine scenario, we select this period to be one year.

The calculated ^{131}I dose rates to regular and maintenance workers at the WWTP for a 1-year integration period are 4.8 × 10^{-10} and 7.9 × 10^{-11} Sv y^{-1}, respectively. For exposure to the public through the

freshwater pathways, the dose rates from external gamma (riverbank occupancy), fish ingestion, drinking WWTP-processed water and drinking unfiltered river water are 1.8×10^{-9}, 2.9×10^{-12}, 6.3×10^{-10} and 1.1×10^{-12} Sv y^{-1}, respectively. Dose rates from ingesting green and root vegetables upon irrigation of farmland are 3.2×10^{-13} and 8.3×10^{-13} Sv y^{-1}, respectively. Finally, the dose rate arising from the use of WWTP sludge in agriculture is 4.6×10^{-12} Sv y^{-1}. All these dose rates are significantly below the trivial dose level of 10 μSv y^{-1}.

8 Conclusions

We have developed a methodology to dynamic calculate dose rates to non-human biota at the outlet of a WWTP for short-lived hospital-sourced radionuclides, based on the biokinetic model D-DAT. We have also developed a method to calculate doses to WWTP workers and from agricultural practices in equilibrium conditions over a 1-year integration period. The scenario chosen was the Molse Nete River in Belgium in low-flow conditions, one of the most relevant in dose terms (even though it is a low dose situation).

We made a series of conservative assumptions, chiefly among them that due to maintenance in the WWTP, the hospital effluents from the decay tanks are bypassed directly into the river for non-human biota, but for humans we assumed a realistic retention efficiency by the WWTP in order to not underestimate dose rates to workers and the agricultural impact of the radioactivity due to irrigation and the use of sewage sludge as a fertiliser. Additionally, a spike release of one MBq of ^{131}I directly into the sewer system was used as a case for unplanned release, to simulate the accidental disposal of an iodate pill into the sewer system. This release can be scaled up or down to suit any kind of accidental situation, given the proportionality between dose rate and the activity released.

All dose rates calculated are low. In the case of biota, they do not exceed the ERICA predicted no effects dose rate of 10 μGy h^{-1}, meaning that no effects are expected at the population level for the fauna and flora in the Molse Nete River (and, by extension, in the other Belgian cases where the generalised concentrations of hospital-released radionuclides tend to be lower). For humans, the dose rates computed for the different exposure pathways are substantially below the 2.4 mSv y^{-1} public dose rate for all natural sources. In most cases, they are also below what is considered a trivial dose (10 μSv y^{-1}). Nevertheless, we consider it as scientifically relevant to continue to perform and refine this type of assessments and to bring down uncertainty in model parameters, given that discharges of radiopharmaceuticals in rivers are on the increase and that it is necessary to explicitly demonstrate to the stakeholders that the public and the environment are protected from their effects.

The approach used here can be considered a screening approach and, as such, can be subject to future improvement. We recommend experimental biokinetic research in the form of aquatic tank experiments with freshwater biota, aiming at establishing transfer parameters (concentration factors and biological half-lives of elimination) for the radionuclides for which the data are not available and had to be deduced by applying extrapolation methods. The main candidate here is ^{201}Tl, which appears to be a main contributor to dose among the various radionuclides hereby considered.

For the WWTP pathway, the main uncertainty is in the retention efficiencies for the different waste streams, whereupon we have adopted generic data but in practice further study could be done on a more case-specific basis. Further refinement of the dose calculations at the WWTP is also possible, in particular regarding (a) the working pattern at the plant in terms of occupancy fractions, (b) establishing the transit times of the different source term fractions through the plant and further afield and (c) factorising realistic shielding conditions which in practice must result in much lower doses to the workers. Another, more general kind of uncertainty is the physico-chemical behaviour of radiopharmaceuticals in the environment (Vives i Batlle et al., 2022).

Looking into the future, a pan-European screening assessment approach with possibility to enter site-specific information could be developed as part of a future project, so that different member states

can be in a position to perform and compare assessments of the impact of radiopharmaceuticals on people and the environment using a consistent methodology.

9 Acknowledgements

10 References

Adamatzky, A. (2001) ModelMaker. Kybernetes 30, 120-125.

Beresford, N.A., Beaugelin-Seiller, K., Burgos, J., M., C., Fesenko, S., Kryshev, A., Pachal, N., Real, A., Su, B.S., Tagami, K., Vives i Batlle, J., Vives-Lynch, S., Wells, C., Wood, M.D. (2015a) Radionuclide biological half-life values for terrestrial and aquatic wildlife. Journal of Environmental Radioactivity 150, 270-276.

Beresford, N.A., Beaugelin-Seiller, K., Wells, C.V.-L., S., Vives i Batlle, J., Wood, M.D., Tagami, K., Real, A., Burgos, J., Fesenko, S., Cujic, M., Kryshev, A., Pachal, N., Su, B.S., Barnett, C.L., Uchida, S., Hinton, T., Mihalík, J., Stark, K., Willrodt, C., Chaplow, J.S. (2015b) A database of radionuclide biological half-life values for wildlife. NERC-Environmental Information Data Centre. http://dx.doi.org/10.5285/b95c2ea7-47d2-4816-b942-68779c59bc4d.

Blaylock, B.G., Frank, M.L., (1981) Bioaccumulation and distribution of [95m]Tc in an experimental freshwater pond. Report IAEA-SM-257/41. International Atomic Energy Agency, Vienna.

Brown, J., Alfonso, B., Avila, R., Beresford, N., Copplestone, D., Hosseini, A. (2016) A new version of the ERICA tool to facilitate impact assessments of radioactivity on wild plants and animals. Journal of Environmental Radioactivity 153, 141-149.

Brown, J.E., Alfonso, B., Avila, R., Beresford, N.A., Copplestone, D., Pröhl, G., Ulanovsky, A. (2008) The ERICA Tool. Journal of Environmental Radioactivity 99, 1371-1383.

Brown, J.E., Beresford, N.A., Hosseini, A. (2013) Approaches to providing missing transfer parameter values in the ERICA Tool: how well do they work? Journal of Environmental Radioactivity 126, 399-411.

Citra, M.J. (1997) Modelmaker 3.0 for Windows. Journal of Chemical Information and Computer Sciences 37, 1198-1200.

Copplestone, D., Hingston, J.L., Real, A. (2008) The development and purpose of the FREDERICA radiation effects database. Journal of Environmental Radioactivity 99, 1456-1463.

EA, (2022) Initial radiological assessment tool 2: part 2 methods and input data. Chief Scientist's Group report, Environment Agency, Bristol, 403 pp.

Eckerman, K.F., Ryman, J.C., (1993) External Exposure To Radionuclides In Air, Water, And Soil. Federal Guidance Report No. 12, EPA-402-R-93-081, p. 238 pp.

Fiengo Pérez, F., Sweeck, L., Vives i Batlle, J., (2022) Deliverable D3.4 - Radionuclide dispersion simulations results. Radiation risk appraisal for detrimental effects from medical exposure during management of patients with lymphoma or brain tumour (SINFONIA) Euratom Project 945196, 59 pp.

FREDERICA, (2006) FREDERICA Radiation Effects Database. Available from: http://www.frederica-online.org/mainpage.asp.

Hevland, M.E., (1981) Radiotechnetium as an environmental contaminant: Metabolism by two freshwater species, the pearl mussel (Margaritifera margaritifera) and the roughskinned newt (Taricha granulosa). Master's thesis. Corvallis, Oregon State, University. 64 pp.

IAEA, (2001) IAEA. Generic models for use in assessing the impact of discharges of radioactive substances to the environment. IAEA Safety Reports Series 19. International Atomic Energy Agency, Vienna. Available from https://www.iaea.org/publications/6024/generic-models-for-use-in-assessing-the-impact-of-discharges-of-radioactive-substances-to-the-environment

IAEA, (2010) Handbook of parameter values for the prediction of radionuclide transfer in terrestrial and freshwater environments. Technical Reports Series No. 472. International Atomic Energy Agency, Vienna. Available from https://www-pub.iaea.org/mtcd/publications/pdf/trs472_web.pdf [Accessed 22 Oct. 2020], Vienna.

IAEA, (2014) Radiation Protection and Safety of Radiation Sources: International Basic Safety Standards. IAEA Safety Standards Series No. GSR Part 3, International Atomic Energy Agency, Vienna, 436 pp.

ICRP, (1996) ICRP Publication 72: Age-dependent Doses to the Members of the Public from Intake of Radionuclides: Part 5. Compilation of Ingestion and Inhalation Dose Coefficients. International Commission on Radiological Protection, Pergamon Press, Oxford.

ICRP, (2008) Environmental Protection: The Concept and use for Reference Animals and Plants.International Commission on Radiological Protection Publication 108, Annals of the ICRP 38(4-6), Elsevier Ltd., 76 pp.

ICRP, (2012) ICRP Publication 119: Compendium of Dose Coefficients based on ICRP Publication 60. C.H. Clement (Ed.), Annals of the ICRP 41(1), 129 pp.

ICRP (2017) Dose Coefficients for Non-human Biota Environmentally Exposed to Radiation. International Commission on Radiological Protection Publication 136. Annals of the ICRP 46, 1-136.

Lepicard, S., Heling, R., Maderich, V. (2004) POSEIDON/RODOS models for radiological assessment of marine environment after accidental releases: application to coastal areas of the Baltic, Black and North Seas. Journal of Environmental Radioactivity 72, 153-161.

Lepicard, S., Raffestin, D., Rancillac, F. (1998) POSEIDON: A dispersion computer code for assessing radiological impacts in a European sea water environment. Radiation Protection Dosimetry 75, 79-83.

Mahmood, Z.U.W., Norfaizal, M., Abu Bakar, N.S., (2014) Laboratory Bioaccumulation, Depuration And Total Dose Rate Of Waterborne Th-232 In Freshwater Fish Of Anabas Testudineus. In: Research and Development Seminar 2014; Bangi (Malaysia), 14-16 Oct 2014. Oral presentation.

McDonnell, C.E., (2004) Radiological assessments for small users. National Radiation Protection Board Report NRPB-W63, United Kingdom, 95 pp.

McKenzie-Carter, M., (1985) Uptake and retention of technetium by two freshwater species, the crayfish Pacifastacus leniusculus and the snail Juga silicula. Thesis for the degree of Master of Science in General Science (Radiation Health), Oregon State University, 66 pp.

Rigas, M.L. (2000) Software Review: Modelmaker 4.0. Risk Analysis 20, 543-544.

Seaman, J.C., Kaplan, D.I., (2010) Chloride, Chromate, Silver, Thallium and Uranium Sorption to SRS Soils, Sediments, and Cementitious Materials. Report SRNL-STI-2010-00493, Savannah River National Laboratory, Aiken, SC, 18 pp.

Simmonds, J.R., Bexon, A.P., Lepicard, S., Jones, A.L., Harvey, M.P., Sihra, K., S.P., N., (2004) Update of the MARINA Project on the radiological exposure of the European Community from radioactivity in North European marine waters. Annex D: Radiological Impact on EU Member States of Radioactivity in North European Waters. European Commission report, 190 pp.

Sweeck, L., (2018) Element-independent biosphere parameters. Project near surface disposal of category A waste at Dessel. Belgian Agency for Radioactive Waste and Enriched Fissile Materials (NIRAS-ONDRAF) report NIROND-TR 2008–28E V3, 76 pp.

Sweeck, L., (2022) Element dependent environmental input parameters for the biosphere model - Project near surface disposal of category A waste at Dessel. Belgian Agency for Radioactive Waste and Enriched Fissile Materials (ONDRAF/NIRAS) Report NIROND-TR 2008–26E Version 4, 308 pp.

Titley, J.G., Carey, A.D., Crockett, G.M., Ham, G.J., Harvey, M.P., Mobbs, S.F., Tournette, C., Penfold, J.S.S., Wilkins, B.T., (2000) Investigation of the sources and fate of radioactive discharges to public sewers. Environment AgencyTechnical Report EA-RD-TR-P-288, Environment Agency, Bristol, United Kingdom, 274 pp.

Tomczak, W., Boyer, P., Krimissa, M., Radakovitch, O. (2019) K_d distributions in freshwater systems as a function of material type, mass-volume ratio, dissolved organic carbon and pH. Applied Geochemistry 105, 68-77.

UNSCEAR (2000) Sources and effects of ionizing radiation, United Nations Scientific Committee on the Effects of Atomic Radiation, UNSCEAR 2000 Report to the General Assembly with Scientific Annexes, Volume I: Sources, Annex B Exposures from natural radiation source. United Nations, New York. [Available from https://www.unscear.org/docs/publications/2000/UNSCEAR_2000_Annex-B.pdf.

Vives Batlle, J., (2013) Further development of the transfer model D-DAT and of a batch dose calculation tool based on ERICA. Report for COMET Milestone MS-311, Contract Number: Fission-2012-3.4.1-604794, Brussels, 14 pp.

Vives Batlle, J., Wilson, R.C., Watts, S.J., Jones, S.R., McDonald, P., Vives-Lynch, S. (2008) Dynamic model for the assessment of radiological exposure to marine biota. Journal of Environmental Radioactivity 99, 1711-1730.

Vives i Batlle, J. (2016) Dynamic modelling of radionuclide uptake by marine biota: application to the Fukushima nuclear power plant accident. Journal of Environmental Radioactivity 151, 502-511.

Vives i Batlle, J., Aoyama, M., Bradshaw, C., Brown, J., Buesseler, K.O., Casacuberta, N., Christl, M., Duffa, C., Impens, N., Iosjpe, M., Masqué, P., Nishikawa, J. (2018) Marine radioecology after the Fukushima Dai-ichi nuclear accident: Are we better positioned to understand the impact of radionuclides in marine ecosystems? . Science of the Total Environment 618, 80-92.

Vives i Batlle, J., Beresford, N.A., Beaugelin-Seiller, K., Bezhenar, R., Brown, J., Cheng, J.J., Ćujić, M., Dragović, S., Duffa, C., Fiévet, B., Hosseini, A., Jung, K.T., Kamboj, S., Keum, D.-K., Kryshev, A., LePoire, D., Maderich, V., Min, B.-I., Periáñez, R., Sazykina, T., Suh, K.-S., Yu, C., Wang, C., Heling, R. (2016) Inter-comparison of dynamic models for radionuclide transfer to marine biota in a Fukushima accident scenario. Journal of Environmental Radioactivity 153, 31-50.

Vives i Batlle, J., Urso, L., Raskob, W., (2022) Identification and prioritisation of ALLIANCE and NERIS SRA topics relevant to medical radiation protection research. EURAMED Rocc-N-Roll deliverable D2.4, 10 pp.

Vives i Batlle, J., Wilson, R.C., Watts, S.J., Jones, S.R., McDonald, P., Vives-Lynch, S. (2008) Dynamic model for the assessment of radiological exposure to marine biota. Journal of Environmental Radioactivity 99, 1711-1730.

Zitko, V. (1975) Toxicity and pollution potential of thallium. Science of the Total Environment 4, 185-192.